

GMA 08

**Riunione del Gruppo Materiali
dell'AIMETA**

**Genova, Facoltà di Architettura
29 febbraio e 1 marzo 2008**



IL MODELLO DELLA FESSURA COESIVA PER L'ANALISI DEL COMPORTAMENTO MECCANICO DEI MATERIALI

Alberto Carpinteri, Marco Paggi



Politecnico di Torino

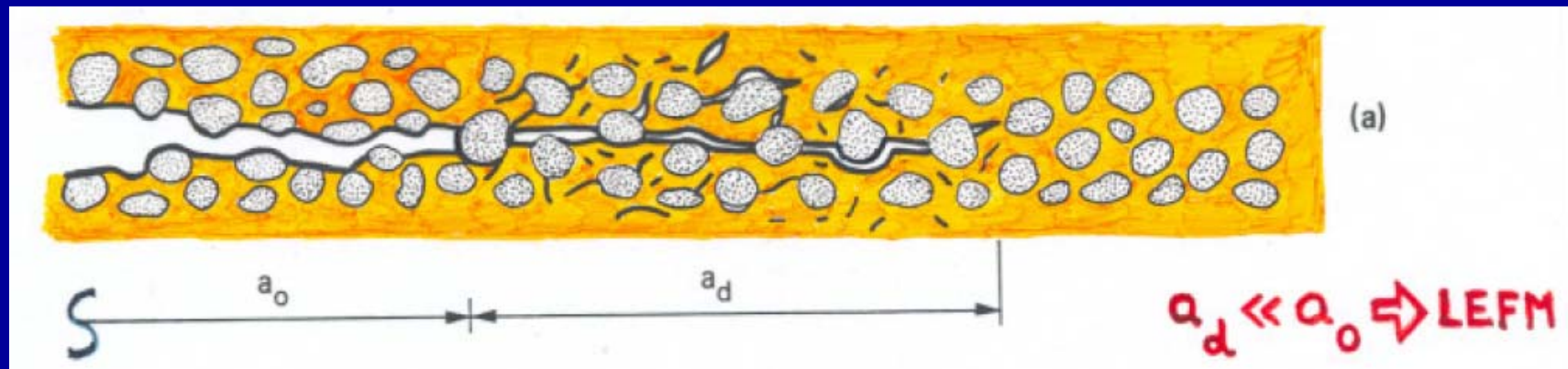
Dipartimento di Ingegneria Strutturale e Geotecnica

Outline

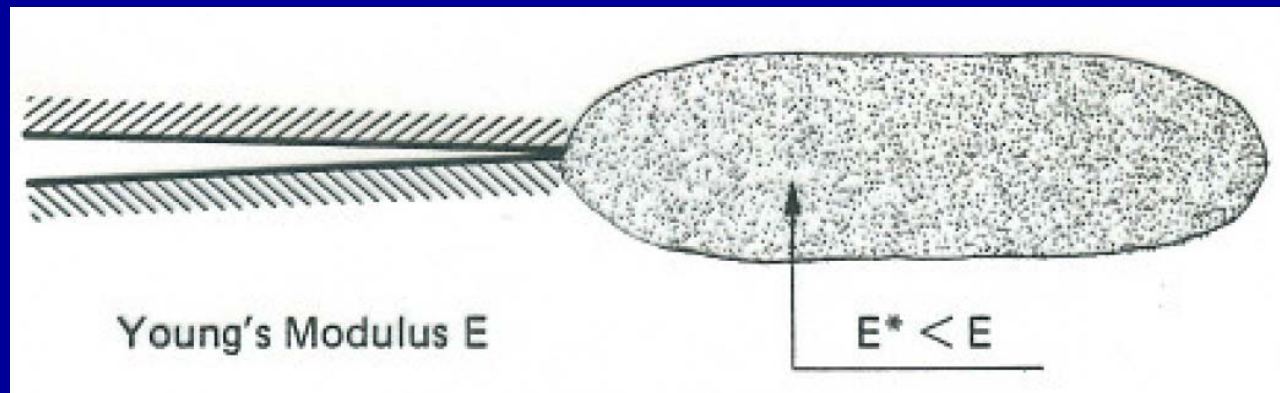
- **Modelling the crack tip process zone in ductile and quasi-brittle materials.**
- **Development of cohesive zone models.**
- **The problem of snap-back instability in structural engineering.**
- **Uniaxial tensile loading of slabs.**
- **Three-point bending beams.**
- **Bifurcation of the global equilibrium (Griffith instability).**
- **Size-scale effects on strength and toughness.**
- **Size-scale transition towards LEFM.**
- **Size-scale transition towards ultimate strength collapse.**
- **Fractal Cohesive Crack Model.**

Modelling the crack tip process zone in ductile and quasi-brittle materials

(a) CRACK TIP PROCESS ZONE

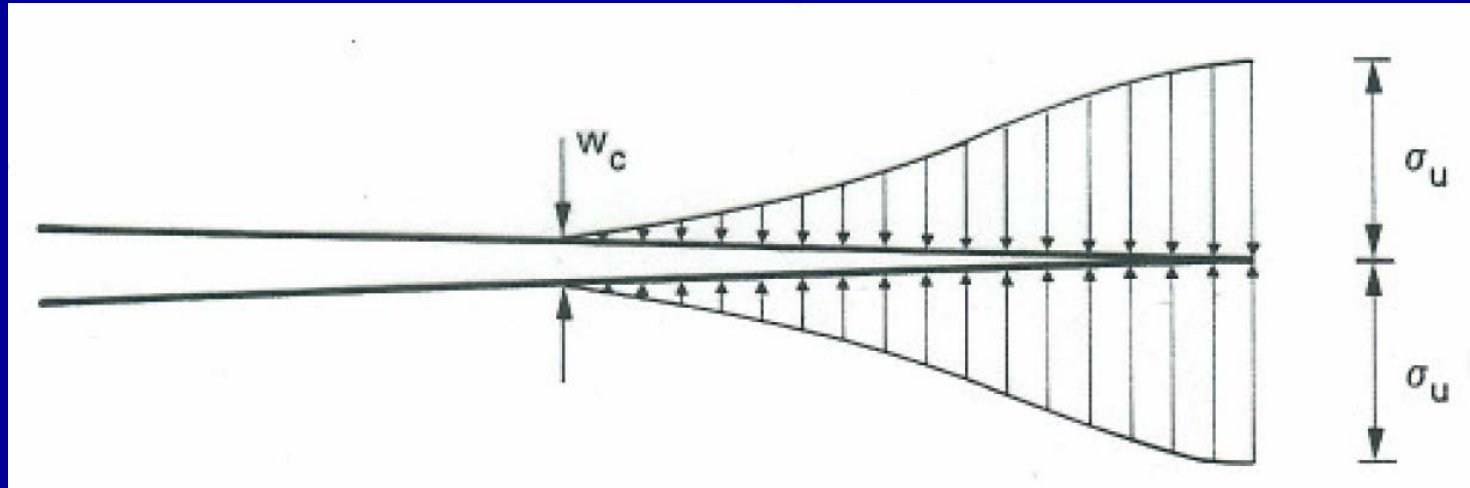


(b) DAMAGE ZONE in front of the real crack tip



**(joint research programme between
Lehigh University and University of Bologna, 1982-83)**

(c) COHESIVE FORCES behind the fictitious crack tip



**(joint research programme between ENEL-CRIS
Milano and University of Bologna, 1983-86)**

Development of Cohesive Zone Models

Dugdale (1960)	crack-tip plastic zone (metals)
Barenblatt (1962)	cohesive atomic forces (crystals)
Bilby, Cottrell & Swinden (1963)	crack-tip plastic zone (metals)
Rice (1968)	crack-tip plastic zone (metals)
Smith (1974)	analysis of different cohesive laws (metals)

Dugdale D.S. (1960) Yielding of steel sheets containing slits, *J. Mech. Phys. Solids* 8:100-114.

Barenblatt G.I. (1962) The mathematical theory of equilibrium cracks in brittle fracture, *Adv. App. Mech.* 7:55-129.

Bilby B.A., Cottrell A.H., Swinden, K.H. (1963) The spread of plastic yield from a notch, *Proc. R. Soc. London* A272:304-314.

Rice J.R. (1968) A path independent integral and the approximate analysis of strain concentration by notches and cracks, *J. Appl. Mech.* 31:379-386.

Smith E. (1974) The structure in the vicinity of a crack tip: a general theory based on the cohesive zone model, *Engng. Fract. Mech.* 6:213-222.

**Hillerborg et al.
(1976)**

**Fictitious Crack Model, for the analysis of
the crack-tip process zone (concrete)**

**Carpinteri
(1984-1989)**

**Cohesive Crack Model, for the analysis of
snap-back instabilities (quasi-brittle mat's)**

Hillerborg A., Modeer M., Petersson P.E. (1976) Analysis of crack formation and crack growth in concrete by means of fracture mechanics and finite element. *Cem. Concr. Res.* 6: 773-782.

Carpinteri A. (1985) Interpretation of the Griffith instability as a bifurcation of the global equilibrium. In: S.P. Shah (Ed.), *Application of Fracture Mechanics to Cementitious Composites* (Proc. of a NATO Adv. Res. Workshop, Evanston, USA, 1984), 284-316. Martinus Nijhoff Publishers, Dordrecht.

Carpinteri A. (1989) Cusp catastrophe interpretation of fracture instability, *J. Mech. Phys. Solids* 37:567-582.

Carpinteri A. (1989) Decrease of apparent tensile and bending strength with specimen size: two different explanations based on fracture mechanics, *Int. J. Solids Struct.* 25:407-429.

Carpinteri A. (1989) Post-peak and post-bifurcation analysis on cohesive crack propagation. *Engng. Fract. Mech.* 32:265-278.

The problem of snap-back instability

Strain softening represents a violation of the Drucker's Postulate. As a consequence, the following phenomena may occur:

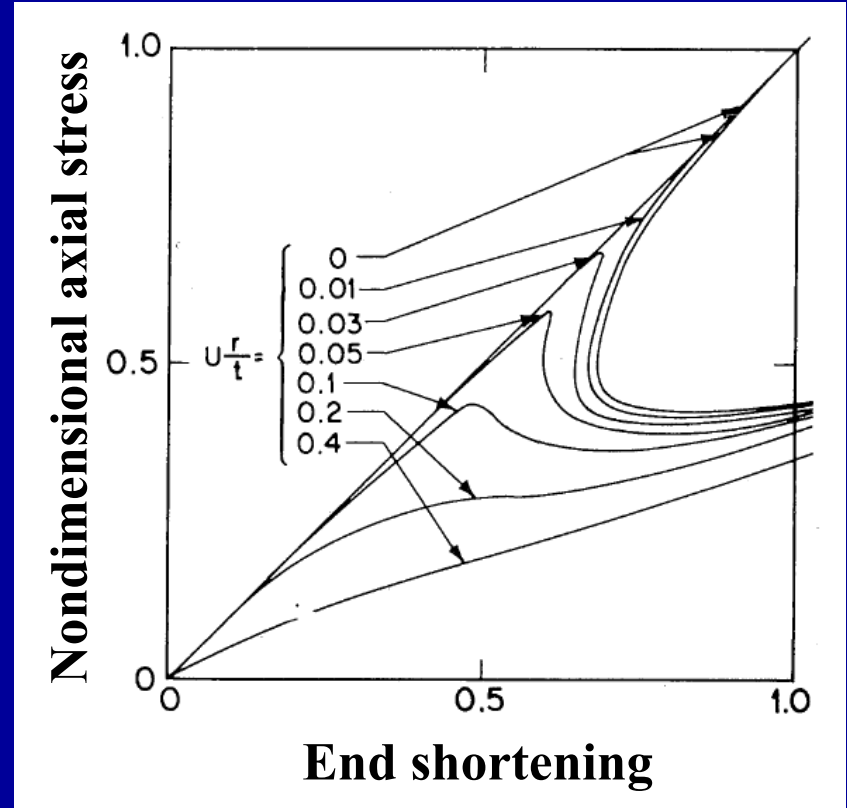
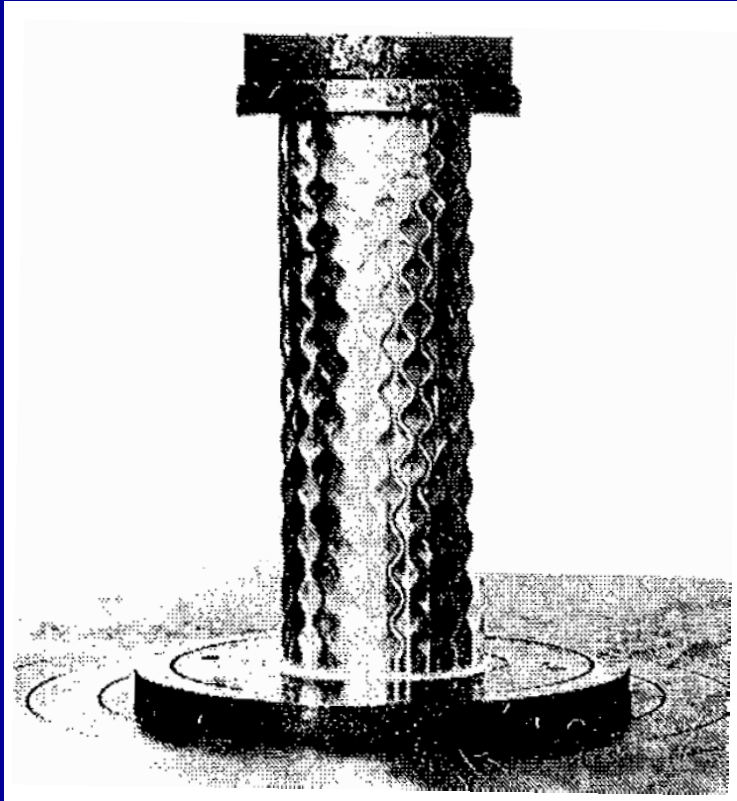
- **Loss of stability in the controlled load condition (*snap-through*);**
- **Loss of stability in the controlled displacement condition (*snap-back*).**
- **Dependence of the results on the type of mesh used in the numerical analyses.**

Maier G. (1966) Behaviour of elastic-plastic trusses with unstable bars, *ASCE J. Engng. Mech.*, **92**:67-91.

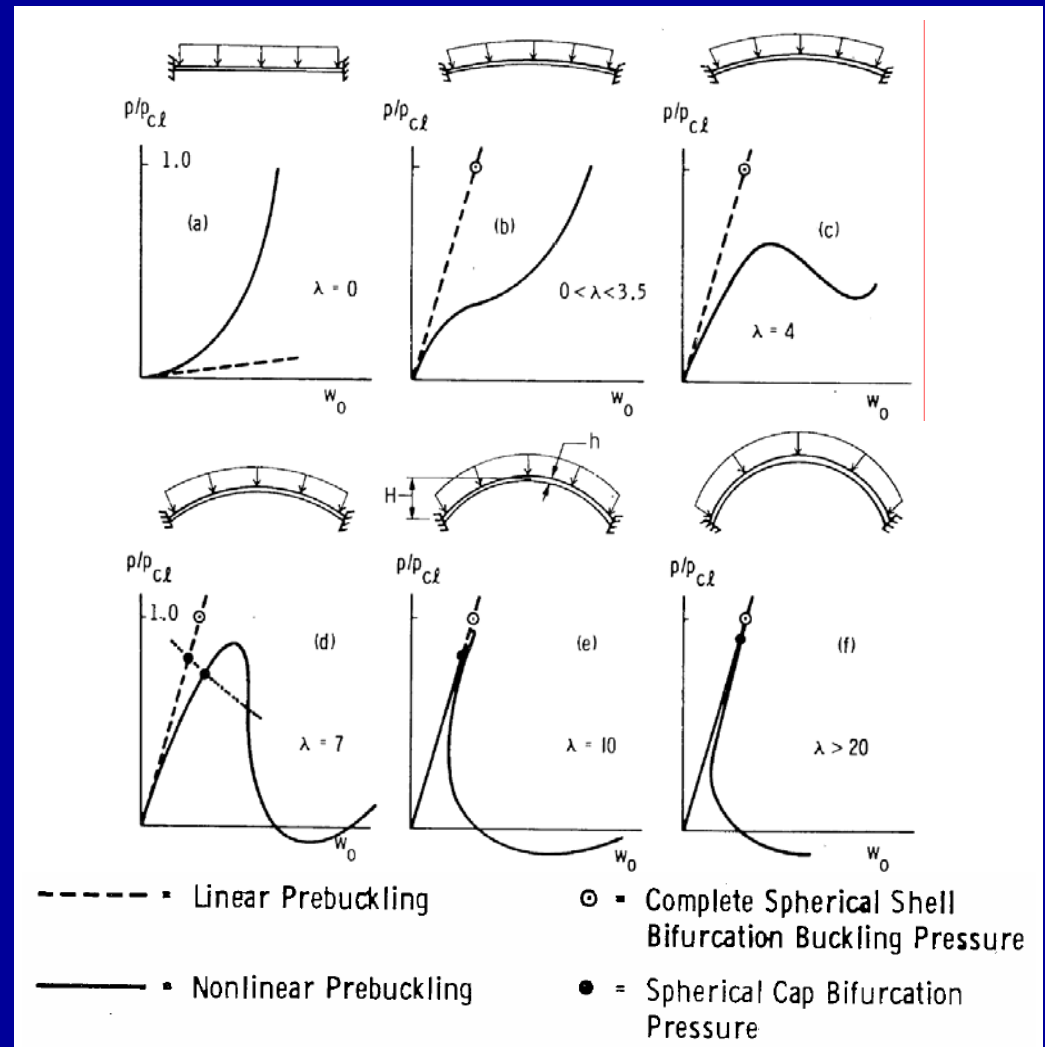
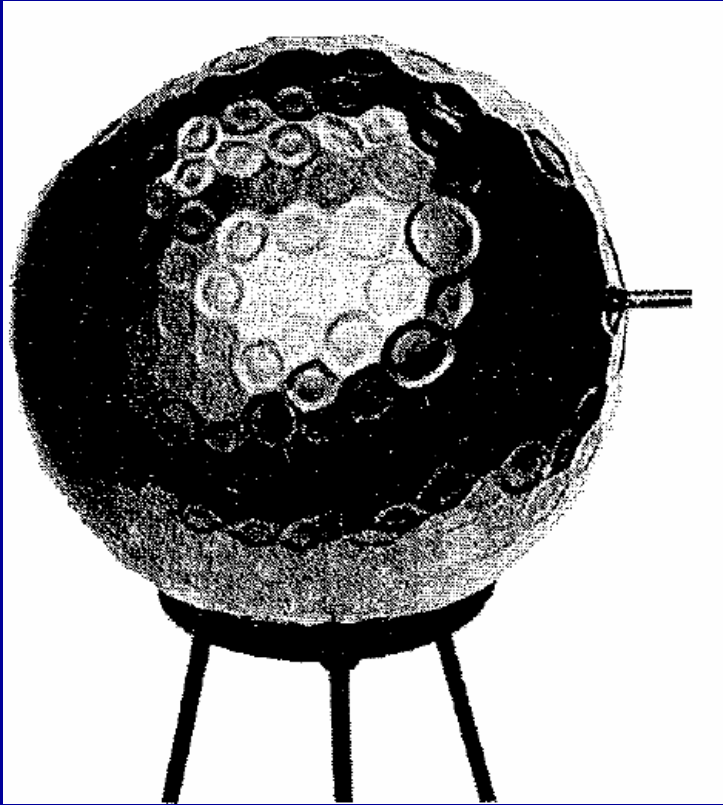
Maier G., Zavelani A., Dotreppe J.C. (1973) Equilibrium branching due to flexural softening, *ASCE J. Engng. Mech.*, **89**:897-901.

Carpinteri A. (1989) Softening and snap-back instability in cohesive solids, *Int. J. Num. Methods Engng.*, **28**:1521-1537.

Snap-back instabilities in thin shells



von Kármán T., Tsien H.S. (1941) The buckling of thin cylindrical shells under axial compression, *J. Aero. Sci.* 8:303-312.



R.L. Carlson, R.L. Sendlebeck and N.J. Hoff (1967) Experimental studies of the buckling of complete spherical shells, *Exp. Mech.* 7:281-288.

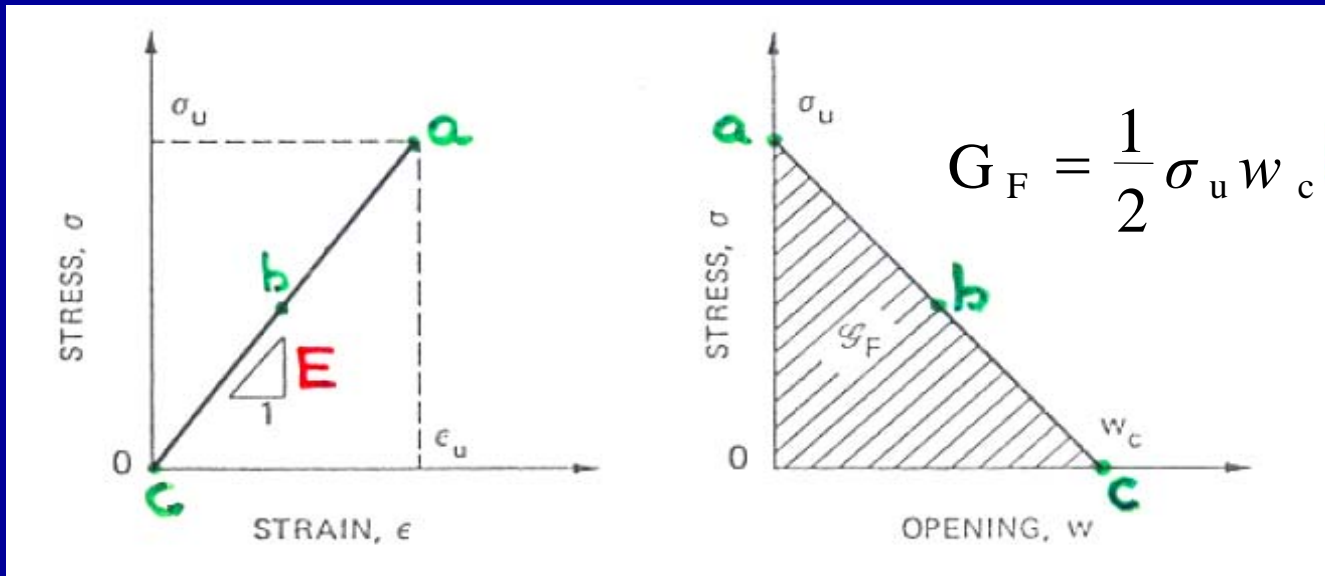
A. Kaplan (1974) Buckling of Spherical Shells, In: *Thin Shell Structures, Theory, Experiment, and Design*, Y.C. Fung and E.E. Sechler (eds.), Prentice-Hall, Inc., Englewood Cliffs, N.J., 248-288.

Uniaxial tensile loading of slabs

$$\sigma = E\varepsilon, \quad \text{for } \varepsilon \leq \varepsilon_u \quad (\text{a})$$

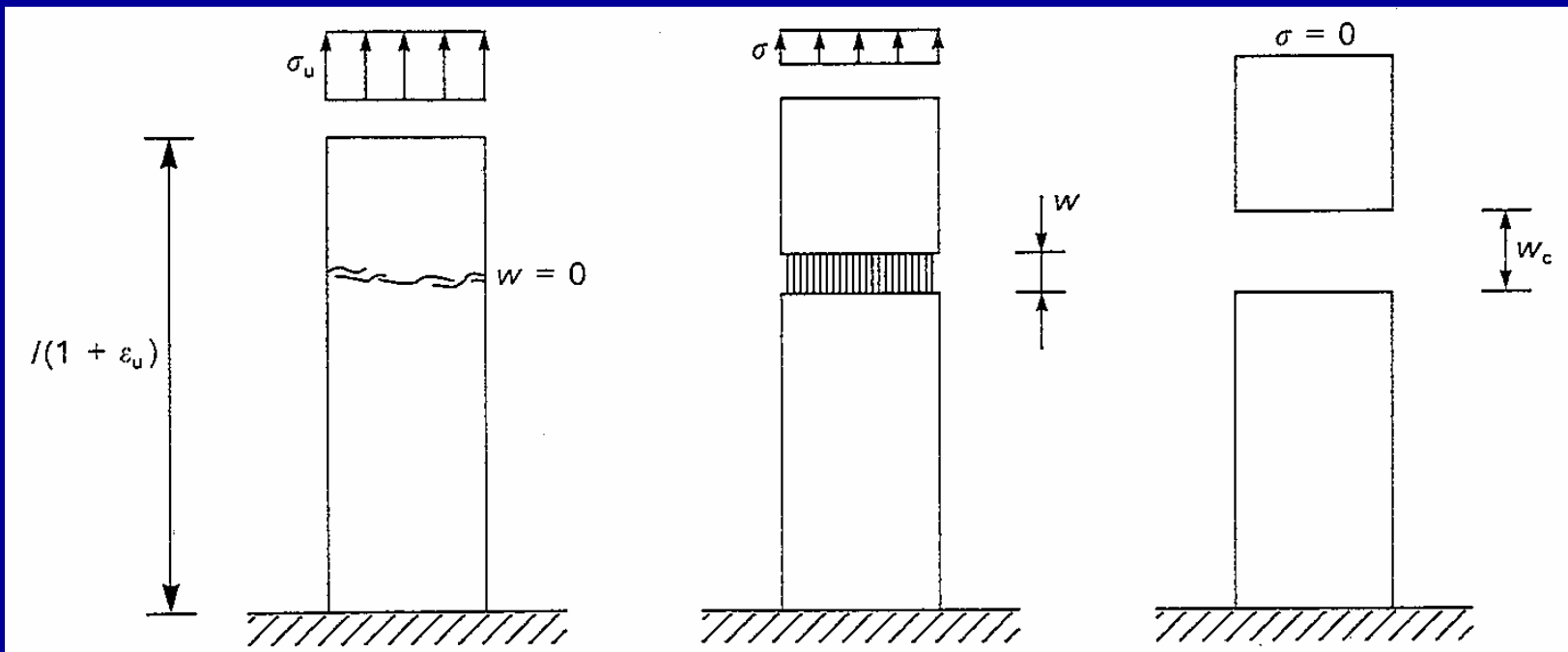
$$\sigma = \sigma_u \left(1 - \frac{w}{w_c} \right), \quad \text{for } w \leq w_c \quad (\text{b})$$

$$\sigma = 0, \quad \text{for } w > w_c$$



(a)

(b)



(a) No damage

(b) Strain localization

(c) Complete separation

(a) $\delta = \frac{\sigma}{E} l,$ for $\varepsilon \leq \varepsilon_u$

(b) $\delta = \frac{\sigma}{E} l + w = \frac{\sigma}{E} l + w_c \left(1 - \frac{\sigma}{\sigma_u} \right),$ for $w < w_c$

(c) $\sigma = 0,$ for $\delta \geq w_c$

Rearranging of Eqs. (a) and (c) we have:

$$(a) \quad \sigma = E \frac{\delta}{l}, \quad \text{for } \delta \leq \varepsilon_u l$$

$$(c) \quad \sigma = 0, \quad \text{for } \delta \geq w_c$$

$$(b) \quad \delta = w_c + \sigma \left(\frac{l}{E} - \frac{w_c}{\sigma_u} \right)$$

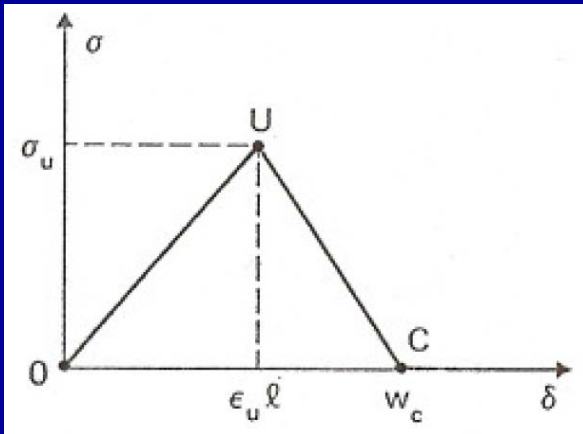
Softening occurs when $d\delta/d\sigma < 0$:

$$\left(\frac{l}{E} - \frac{w_c}{\sigma_u} \right) < 0 \quad \Rightarrow \quad w_c > \varepsilon_u l \quad \text{(softening)}$$

Snap-back takes place when $d\delta/d\sigma \geq 0$:

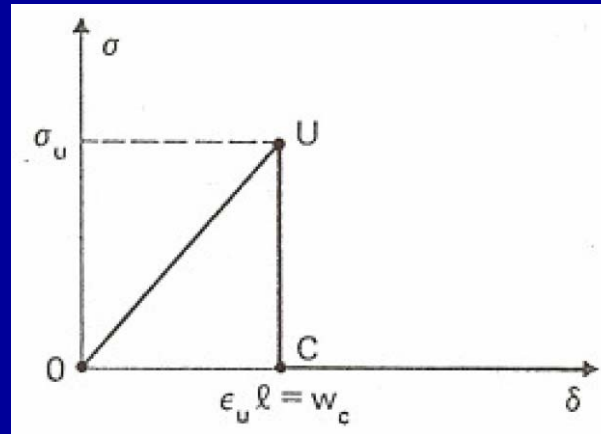
$$\left(\frac{l}{E} - \frac{w_c}{\sigma_u} \right) \geq 0 \quad \Rightarrow \quad w_c \leq \varepsilon_u l \quad \text{(snap-back)}$$

Global stress-displacement response:



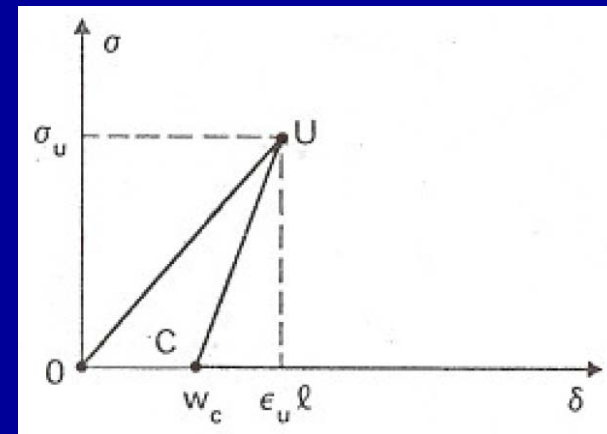
(a)

$w_c > \epsilon_u l$
(softening)



(b)

$w_c = \epsilon_u l$



(c)

$w_c < \epsilon_u l$
(snap-back)

Carpinteri A. (1988) Snap-back and hyperstrength in lightly reinforced concrete beams, *Magazine of Concrete Research*, **40**:209-215.

del Piero G., Truskinovsky L. (1998) A one-dimensional model for localized and distributed failure, *Le Journal de Physique IV*, **8**:95-102.

$$w_c \leq \varepsilon_u l \quad (\text{snap-back condition})$$

$$\frac{(w_c/2h)}{\varepsilon_u (l/h)} \leq \frac{1}{2},$$

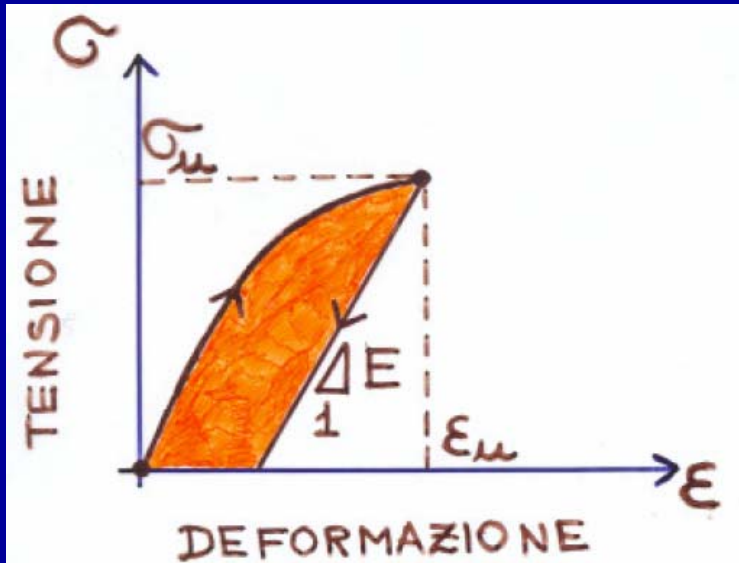
Introducing the energy brittleness number (Carpinteri, 1985):

$$s_E = \frac{w_c}{2h} = \frac{G_F}{\sigma_u h}$$

$$B = \frac{s_E}{\varepsilon_u \lambda} \leq \frac{1}{2} \quad (\text{snap-back condition})$$

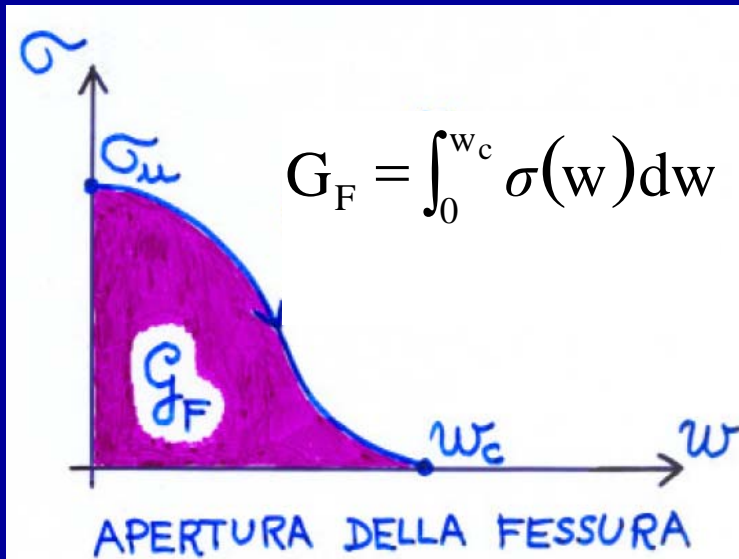
Not the single values of parameters s_E , ε_u and λ , but only their combination $B = s_E / \varepsilon_u \lambda$ is responsible for the global brittleness or ductility of the structure considered.

Fracture energy G_F (J_C integral)



= dissipated energy within the volume

$$\left(\frac{FL}{L^3} = \frac{F}{L^2} \right)$$

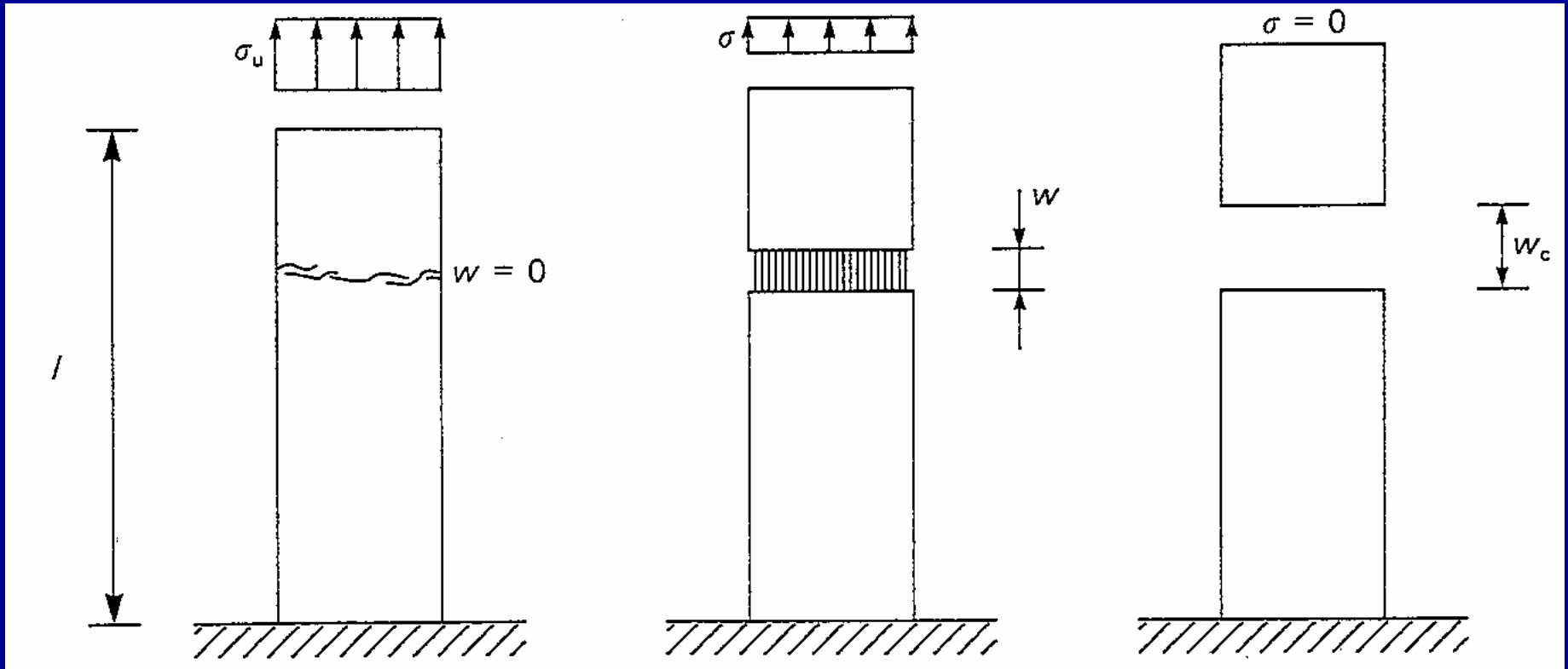


= dissipated energy over the crack surface

$$\left(\frac{FL}{L^2} = \frac{F}{L} \right)$$

$$\text{Dissipated energy} = \text{[Orange Box]} \times \text{Area} \times l + \text{[Purple Box]} \times \text{Area}$$

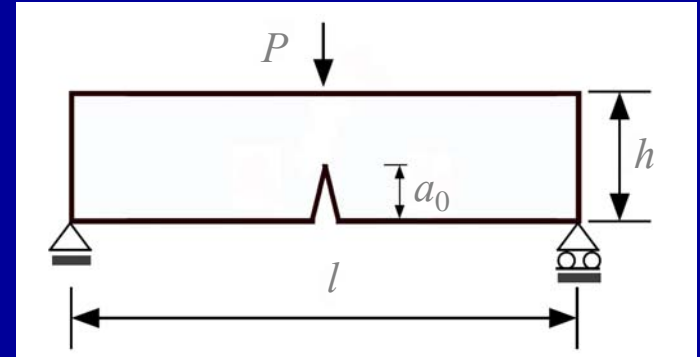
$$\text{Dissipated energy / Area} = \text{[Orange Box]} \times l + \text{[Purple Box]}$$



Three-point bending beams

- **Three Point Bending (TPB) test: specimen behaviour is brittle (snap-back) for:**

- Low fracture toughness, G_F ,
- High tensile strength, σ_u ,
- Large structural size, h .

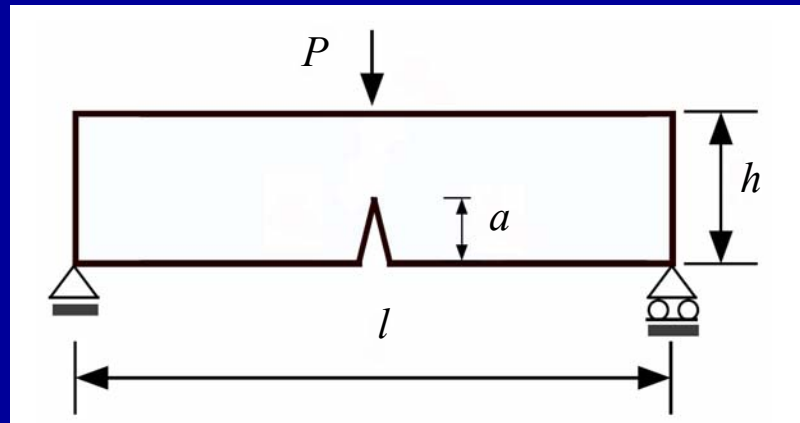


- **This behaviour is synthetically captured by the Brittleness Number s_E :**

$$s_E = \frac{G_F}{\sigma_u h}$$

- **The ductile-brittle transition can be described by the Cohesive Crack Model.**

- Considering a TPB beam, we focus onto two limit situations:
 - (1) $a = 0$: uncracked beam.
 - (2) $a = h$: limit situation of complete fracture with cohesive forces.



$$\tilde{P} = \frac{P}{\sigma_u h^2}$$

Nondimensional load

$$\tilde{\delta} = \frac{\delta}{h}$$

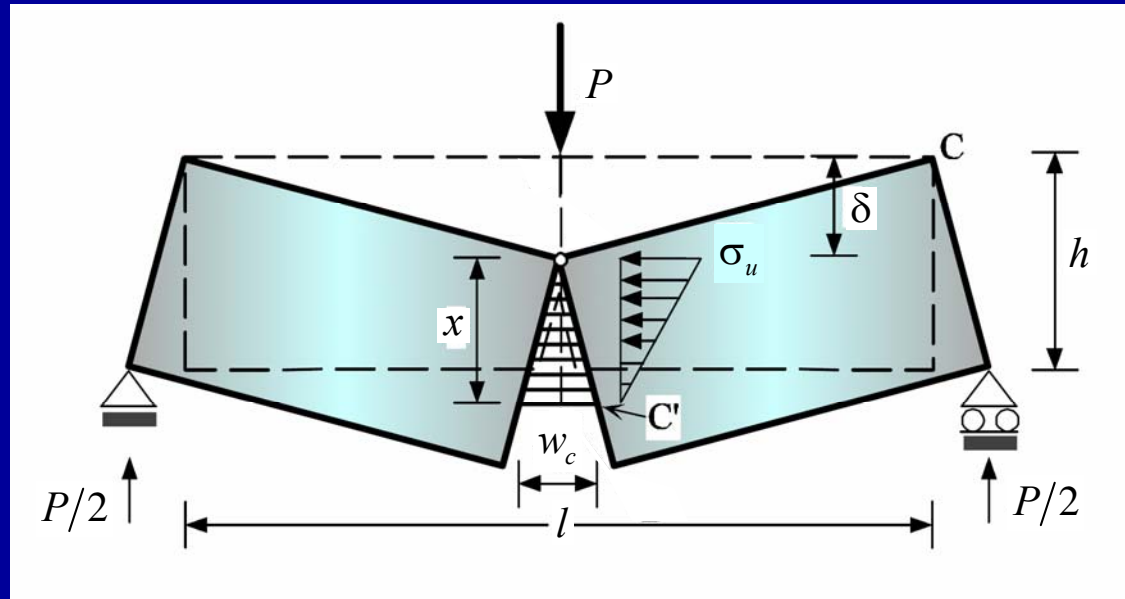
Nondimensional deflection

- **Case 1: $a = 0$**

The load-deflection relation is linear: $\tilde{P} = \frac{4}{\lambda^3} \tilde{\delta}$, for $(\sigma \leq \sigma_u)$ $\tilde{P} \leq 2/3$

- **Case 2: $a = h$**

The following equilibrium scheme can be considered:



The load-deflection relation is hyperbolic:

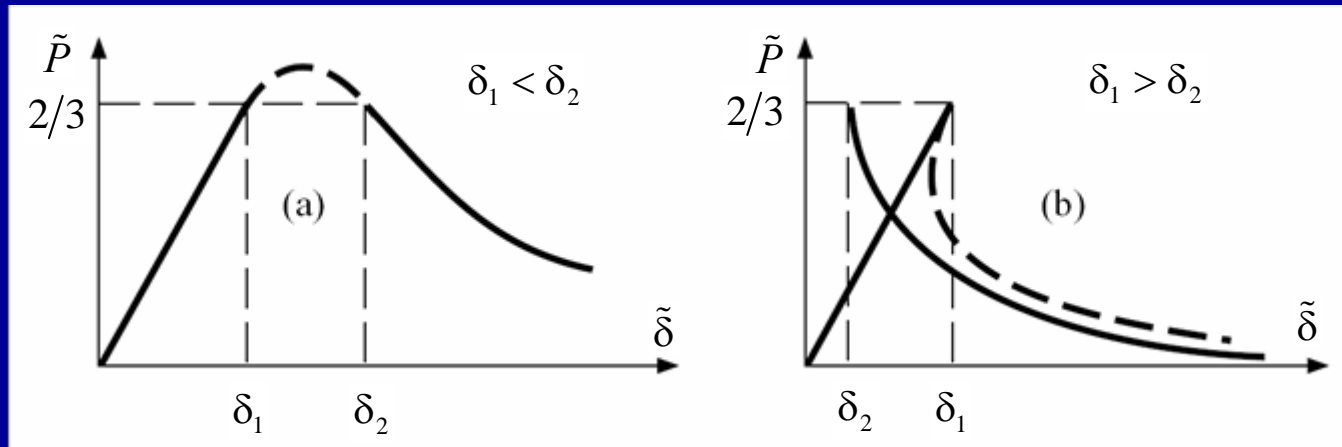
$$\tilde{P} = \frac{1}{6} \left(\frac{S_E \lambda^2}{\varepsilon_u \tilde{\delta}} \right)^2, \text{ for } \tilde{P} \leq 2/3 \quad (x \leq h)$$

Both equations have the same upper limit: $\tilde{P} \leq 2/3$.

- By transforming the load bounds into deflection bounds, a stability criterion for elastic-softening beams is obtained:

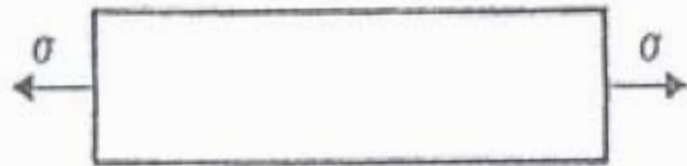
$$\tilde{\delta} \leq \delta_1 = \frac{\lambda^3}{6} \quad (1)$$

$$\tilde{\delta} \geq \delta_2 = \frac{S_E \lambda^2}{2\varepsilon_u} \quad (2)$$

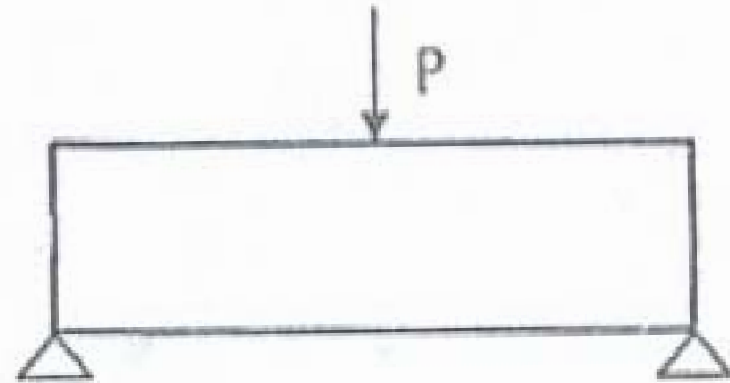


- When the two domains are disjoint, the P - δ curve is regular;
- When they are partially overlapped, it is well-founded to suppose them connected by a curve with highly negative or even positive slope (snap-back).
- Snap-back is thus expected when $\delta_1 > \delta_2 \Rightarrow B = \frac{S_E}{\varepsilon_u \lambda} \leq \frac{1}{3}$.

Unstable behaviour and catastrophic events when:



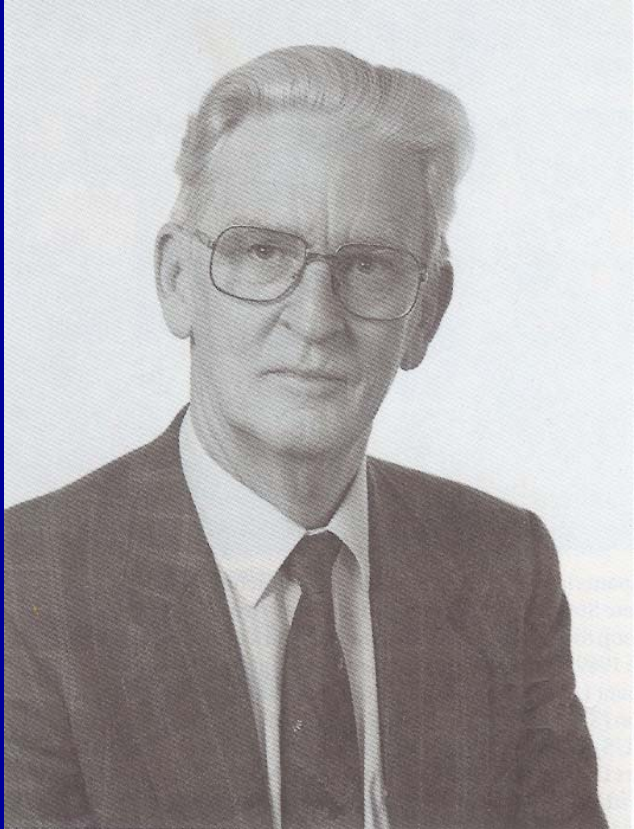
$$B \leq 1/2$$



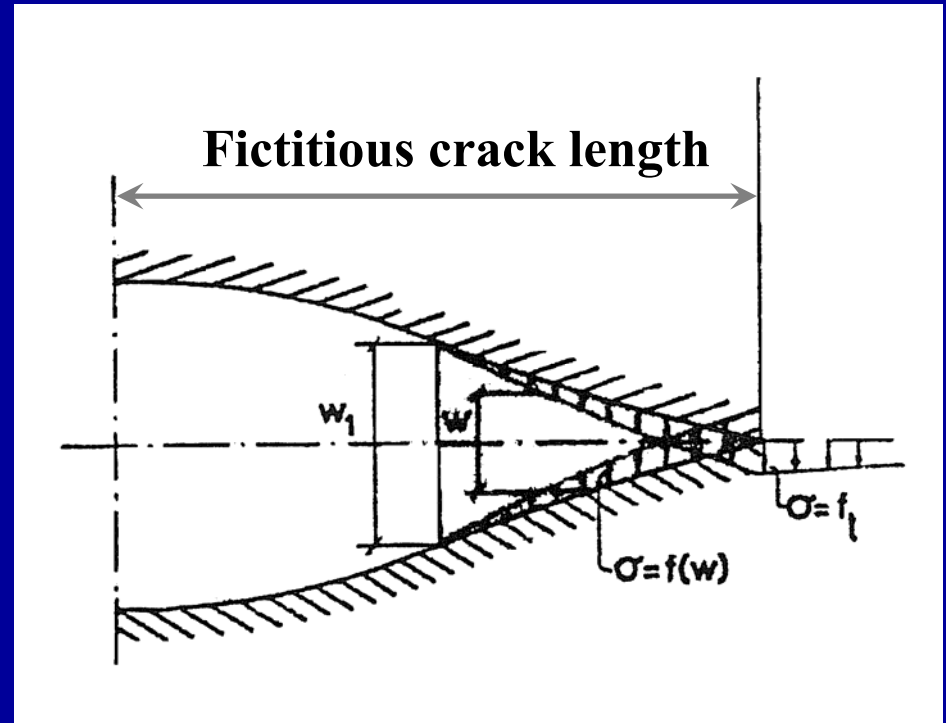
$$B \leq 1/3$$

The relative brittleness of a structure is dependent on loading condition and external constraints.

The Fictitious Crack Model

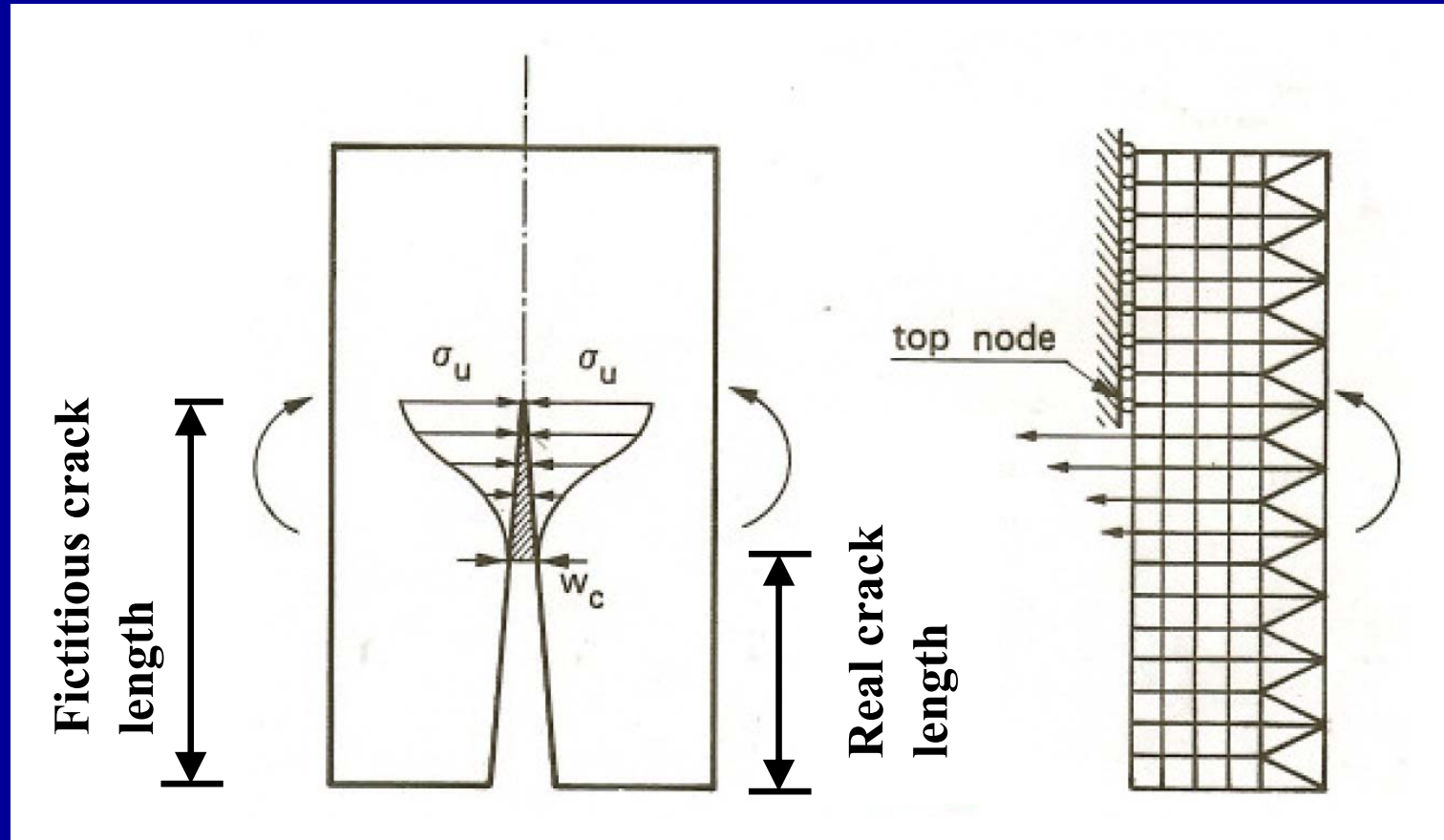


Arne Hillerborg

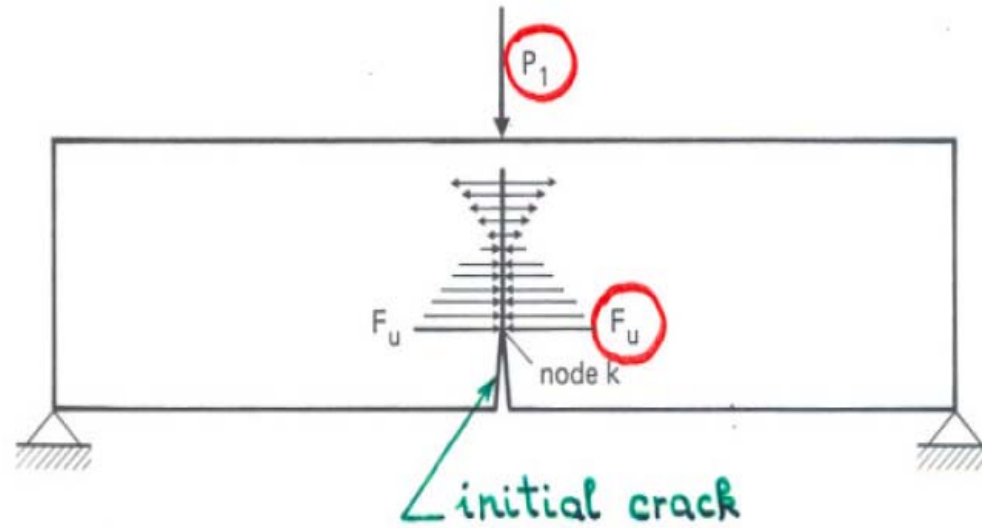
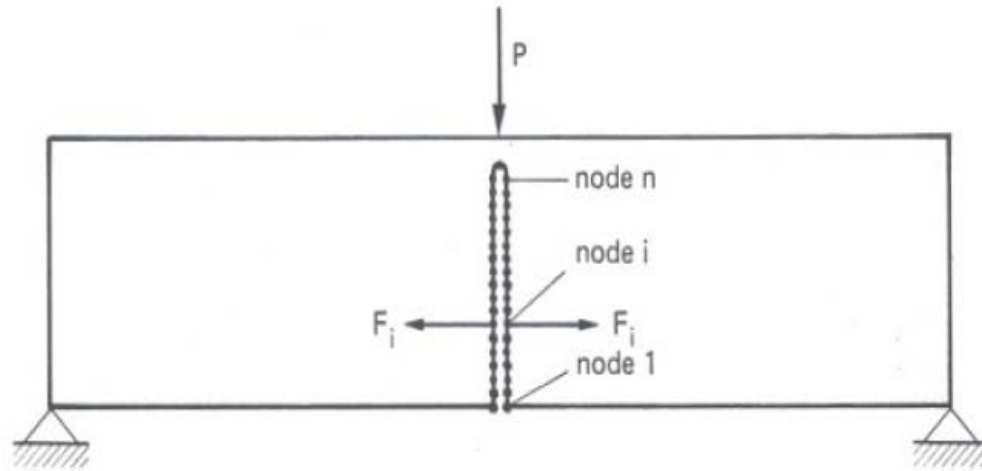


A. Hillerborg, M. Mod er and P.E. Petterson, **Analysis of crack formation and crack growth in concrete by means of fracture mechanics and finite elements**, *Cement and Concrete Research*, Vol. 6, 773-782, 1976.

FRacture ANALysis Code (ENEL-CRIS Milano and University of Bologna)



Carpinteri A. (1985) Interpretation of the Griffith instability as a bifurcation of the global equilibrium. In: S.P. Shah (Ed.), *Application of Fracture Mechanics to Cementitious Composites* (Proc. NATO Adv. Res. Workshop, Evanston, USA, 1984), 284-316. Martinus Nijhoff Publishers, Dordrecht.



$$\{w\} = [K]\{F\} + \{C\}P$$

where: $\{w\}$ = vector of the crack openings

$[K]$ = matrix of the coefficients of influence ($F_i = 1$)

$\{F\}$ = vector of the closing forces

$\{C\}$ = vector of the coefficients of influence ($P = 1$)

$F_i = 0$, for $i = 1, \dots, (k-1)$,

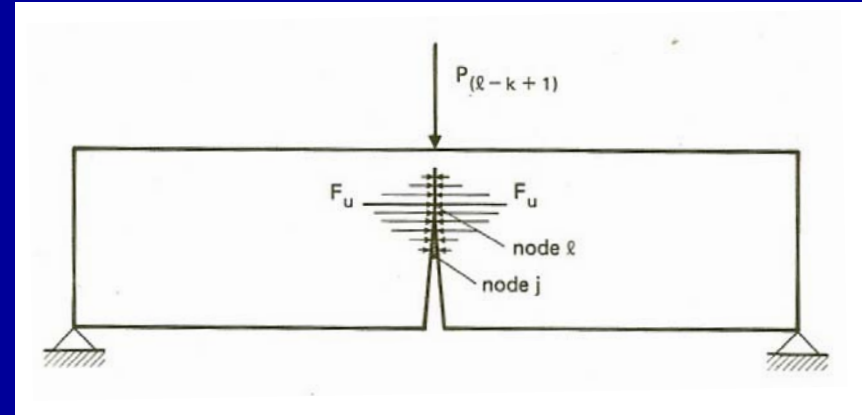
$w_i = 0$, for $i = k, \dots, n$.

2n equations

2n unknowns: $\{w\}$, $\{F\}$

When the process zone is present, between nodes j and l :

$$\begin{cases} F_i = 0, & \text{for } i = 1, \dots, (j-1), \\ F_i = F_u \left(1 - \frac{w_i}{w_c} \right), & \text{for } i = j, \dots, l, \\ w_i = 0, & \text{for } i = 1, \dots, n. \end{cases}$$

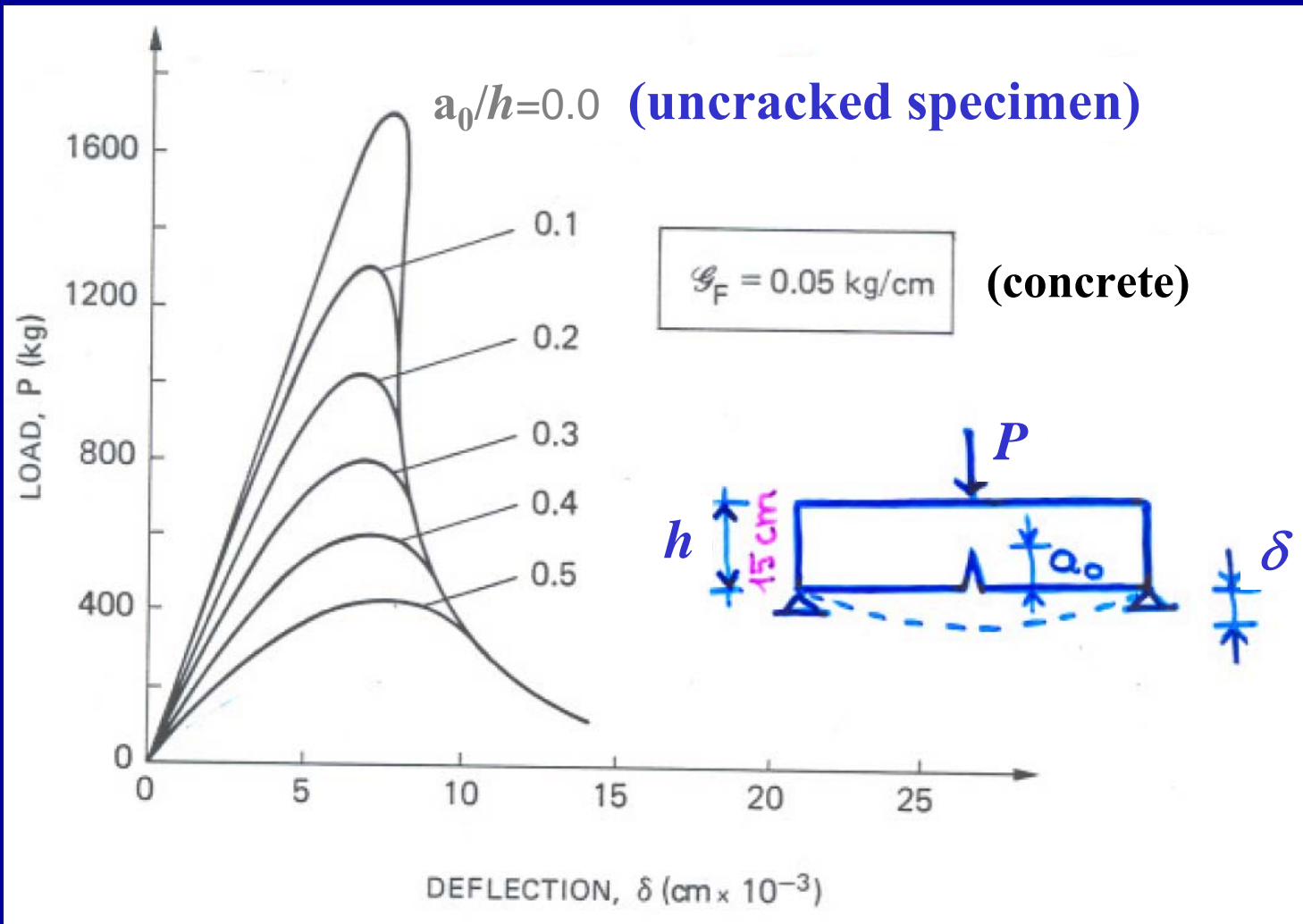


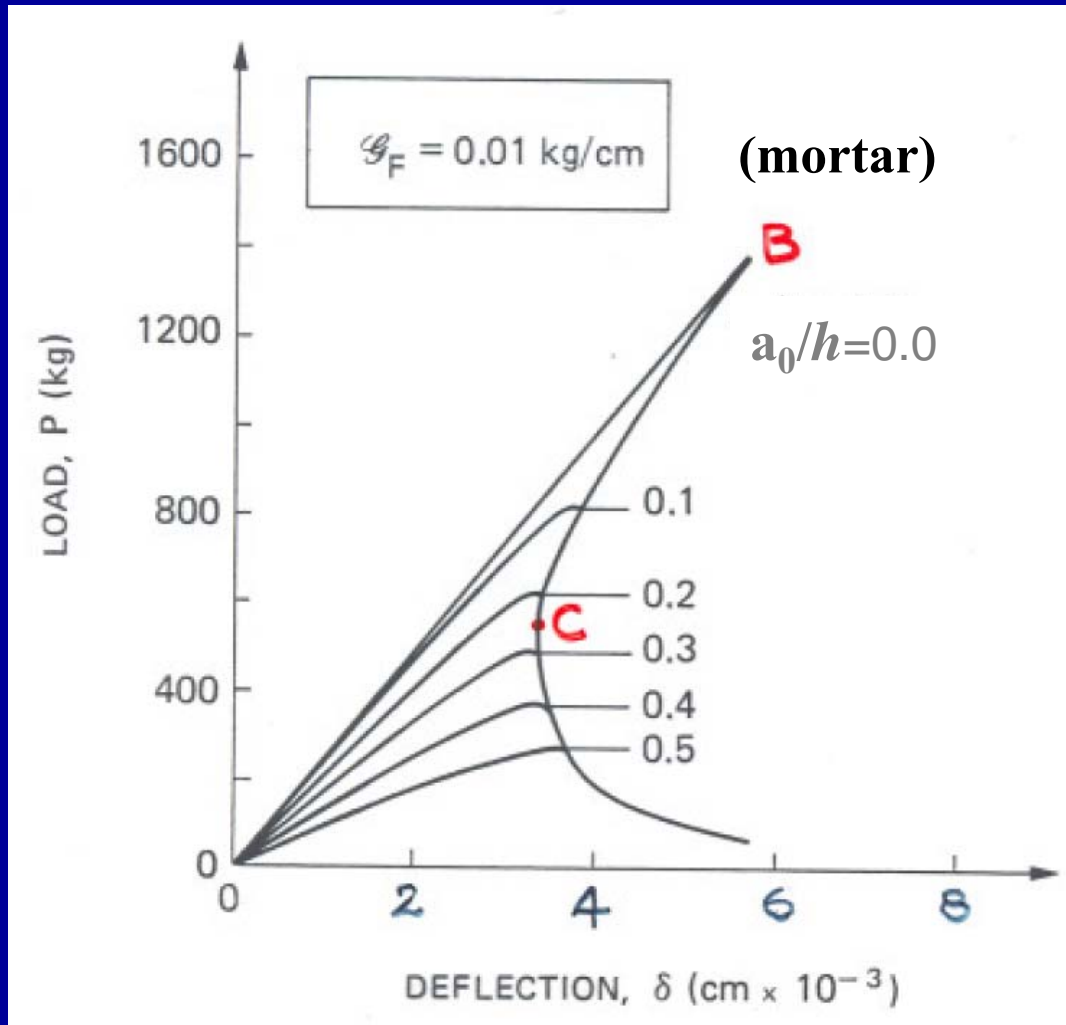
$(2n + 1)$ equations

$(2n + 1)$ unknowns: $\{w\}$, $\{F\}$, P

N.B.: The driving-parameter is the fictitious crack-tip position (Crack Length Control Scheme).

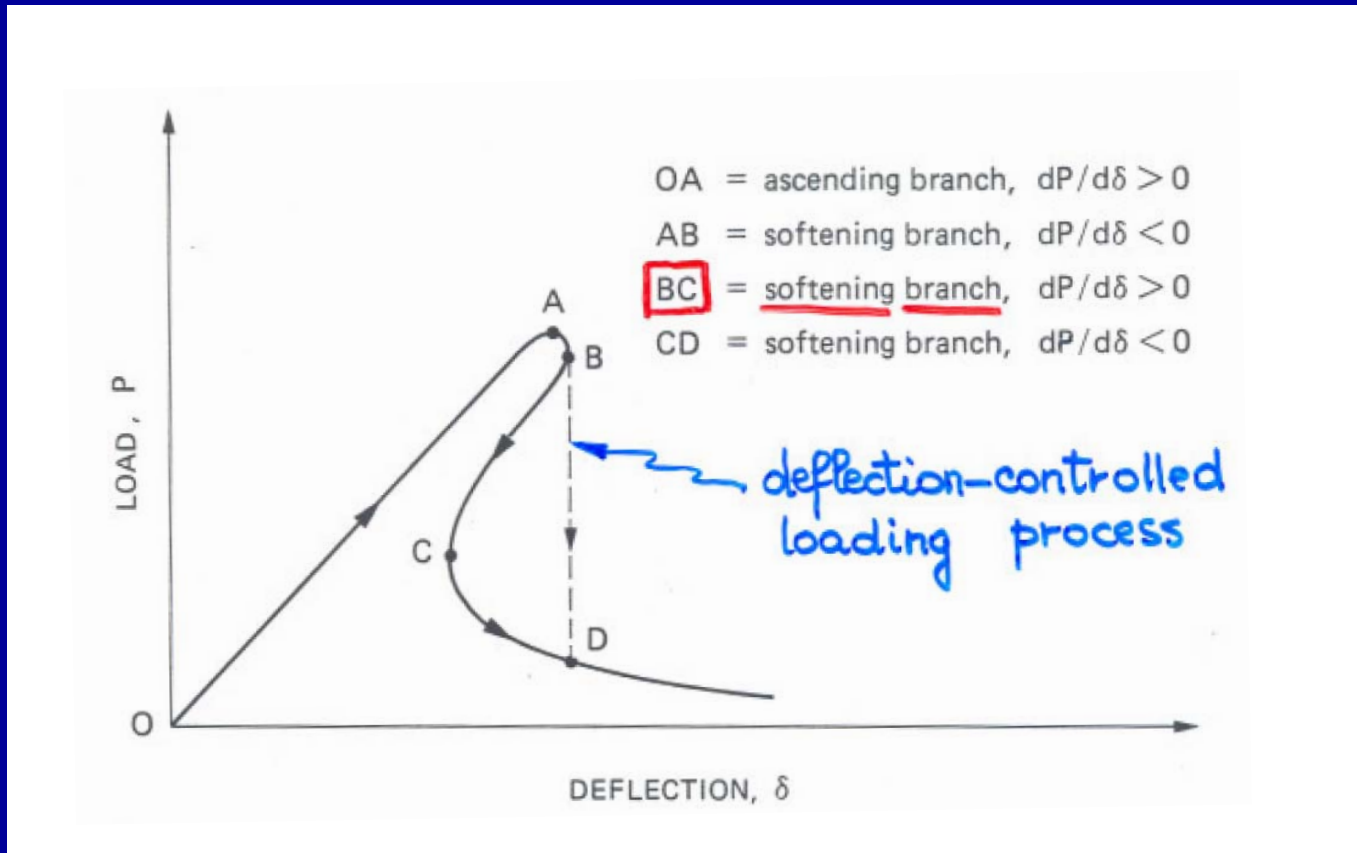
Load-deflection diagrams ($h=15$ cm, notched specimens)



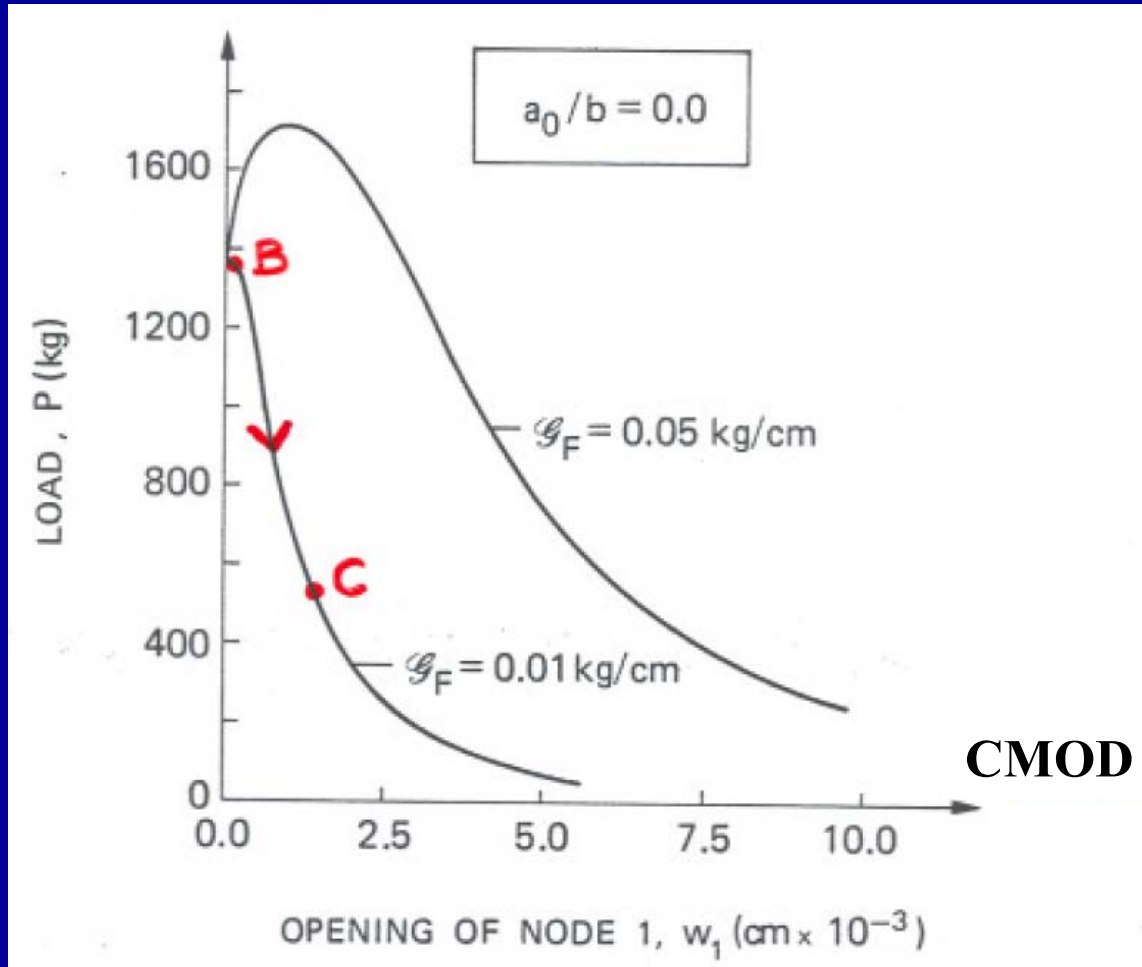


$$a_0/h \leq 0.25 \Rightarrow dP/d\delta > 0 \quad \text{(snap-back)}$$

Bifurcation of the global equilibrium (Griffith instability)

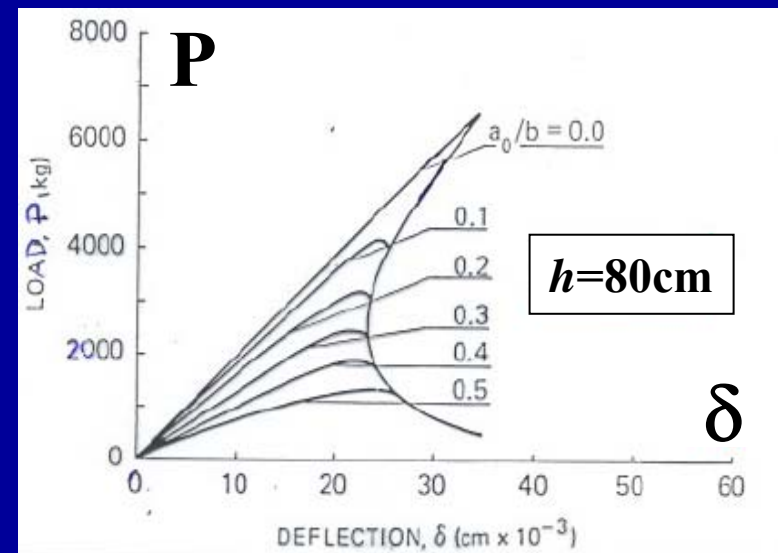
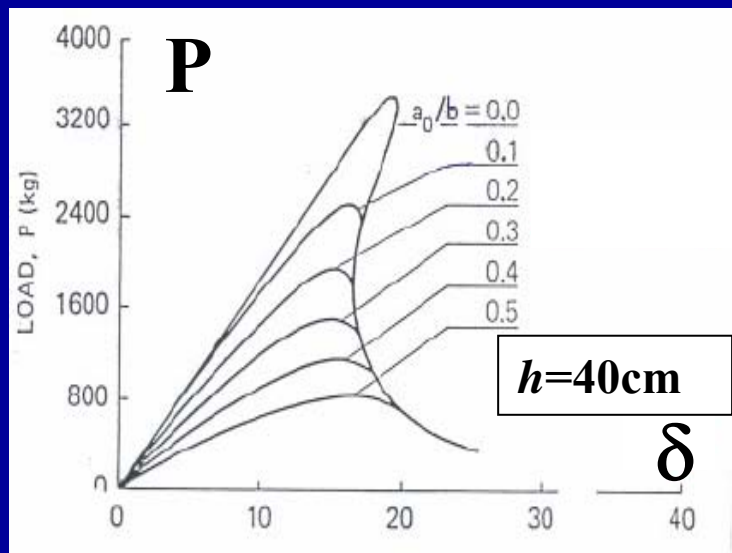
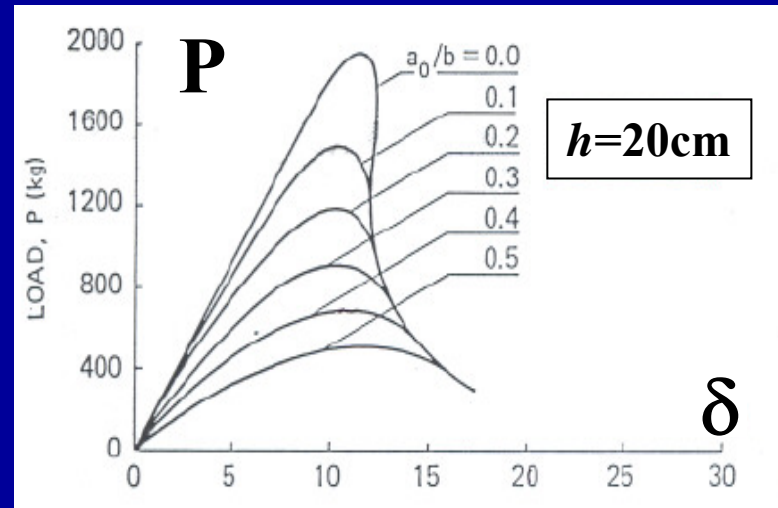
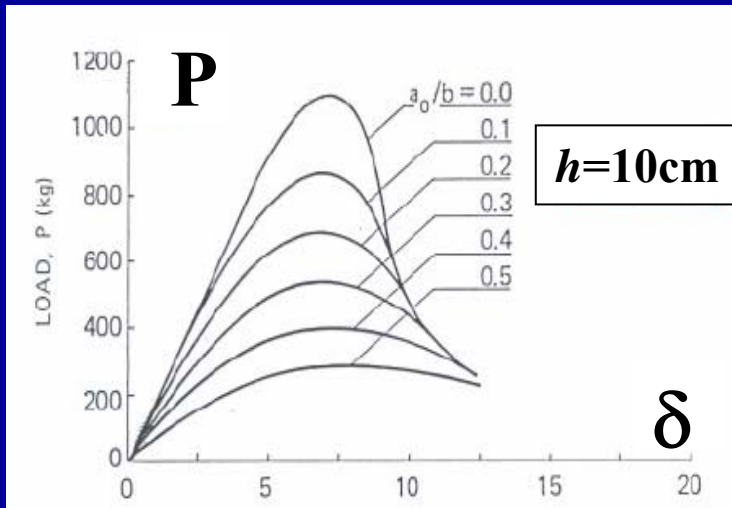


Carpinteri A. (1989) Cusp catastrophe interpretation of fracture instability, *J. Mech. Phys. Solids* 37:567-582.



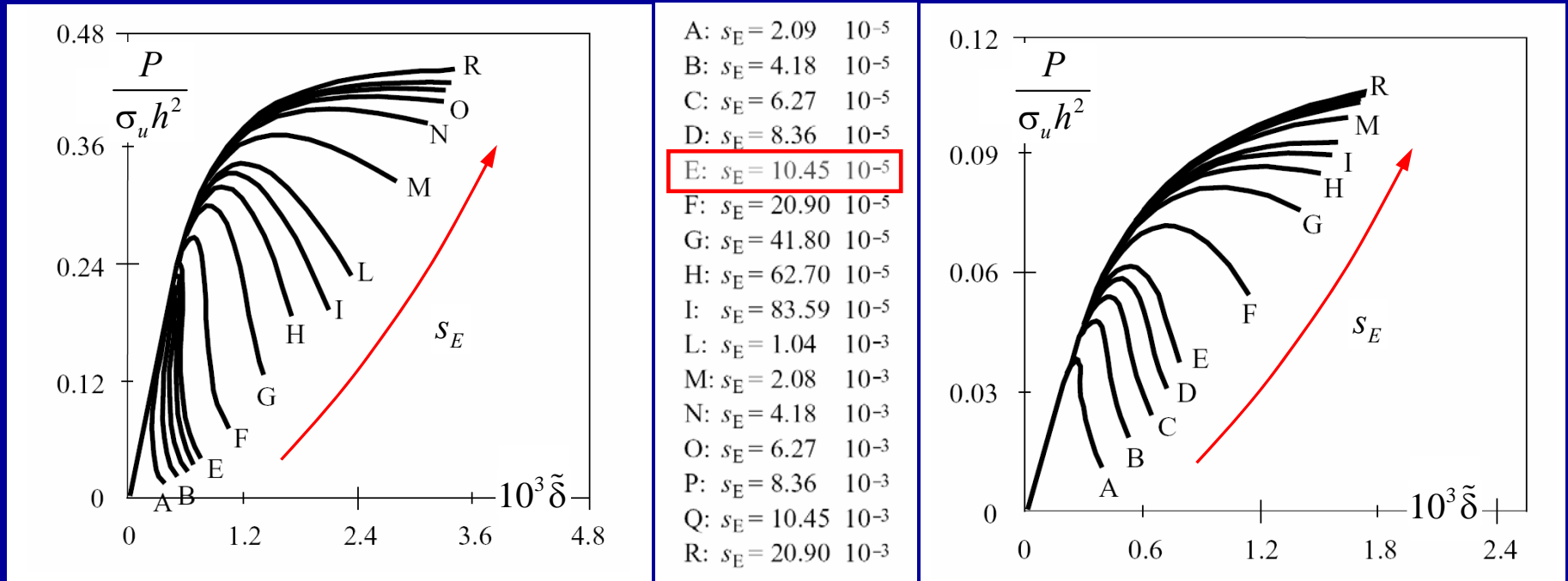
With a CMOD-controlled loading process, it is possible to follow the virtual softening branch BC.

The effect of the structural size-scale



Note the effect of the initial crack length a_0 : the deeper is the crack, the more ductile is the behaviour.

- In a nondimensional plane, the mechanical behaviour is governed by the energy brittleness number (Carpinteri, 1985).



$$a_0/h = 0$$

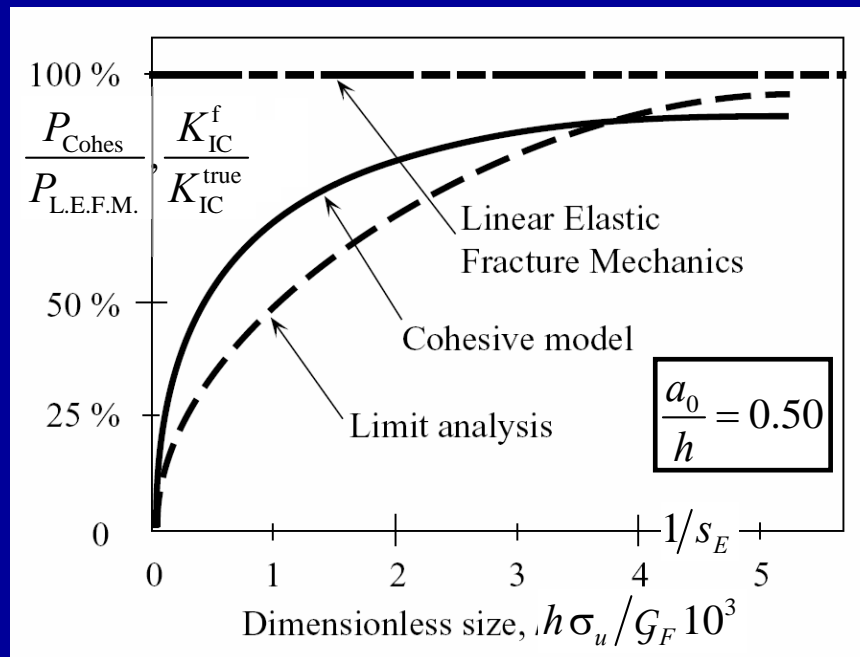
$$a_0/h = 0.5$$

- Snap-back condition:** $B \leq \frac{1}{3} \Rightarrow s_E \leq \frac{\varepsilon_u \lambda}{3} = 11.6 \times 10^{-5}$

$$(\varepsilon_u = 0.87 \times 10^{-4}; \lambda = 4)$$

Size effects on fracture toughness

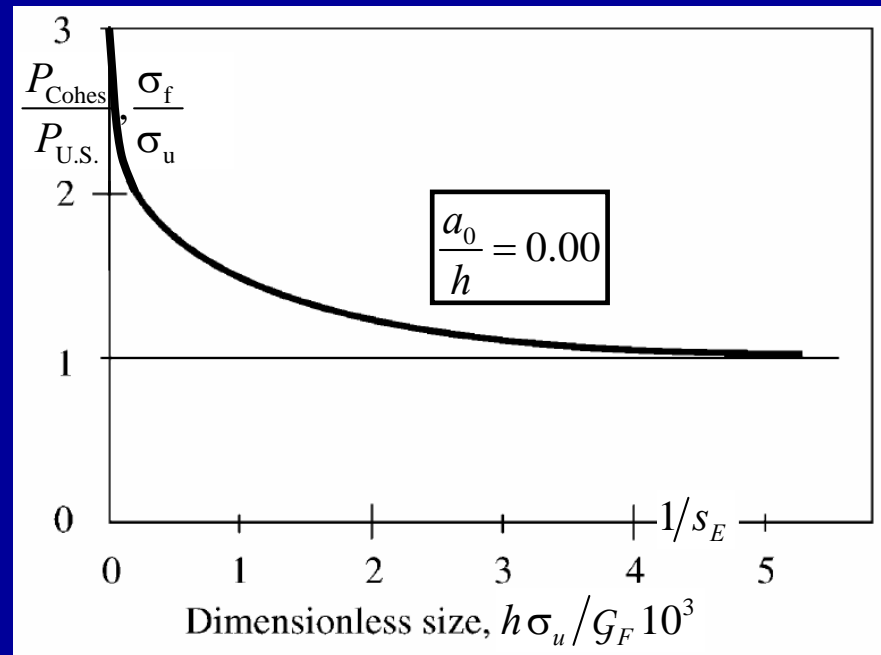
- The ratio $P_{\text{Cohes}}/P_{\text{L.E.F.M.}}$ can be plotted vs. the nondimensional size, $1/s_E$.
- This ratio represents the ratio of the fictitious fracture toughness to the true fracture toughness (considered as a material constant). This ratio converges to unity for very small values of s_E .



- The true fracture toughness, K_{IC} , can be obtained with only very large specimens.

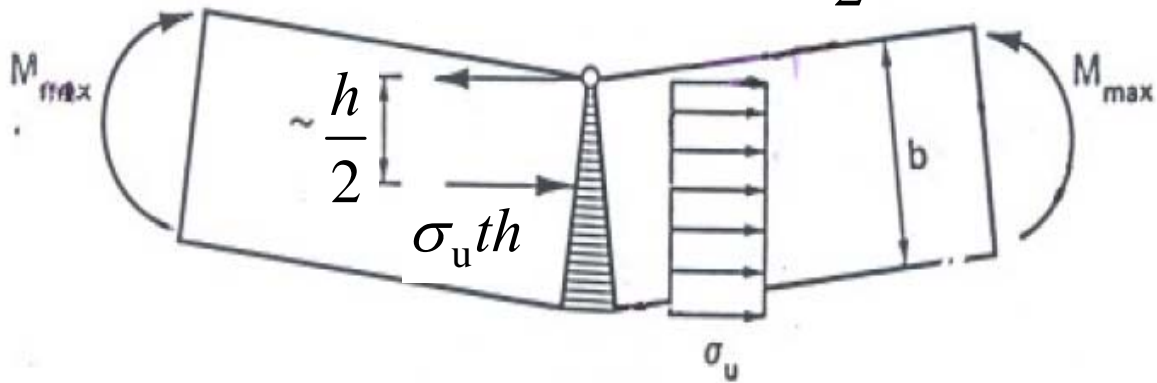
Size effects on tensile strength

- The ratio $P_{\text{Cohes}}/P_{\text{L.E.F.M.}}$ can be plotted against the nondimensional size, $1/s_E$.
- This ratio represents the ratio of the apparent tensile strength to the true tensile strength (considered as a material constant). This ratio converges to unity for very small values of s_E .



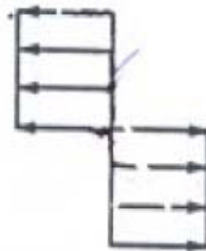
- The true tensile strength, σ_u , can be obtained with only very large specimens.

$$S_E \rightarrow \infty \Rightarrow M_{\max} = (\sigma_u t h) \times \frac{h}{2}$$



$$\sigma_u t \frac{h^2}{2}$$

$$M_P = M_{\max} / 2$$



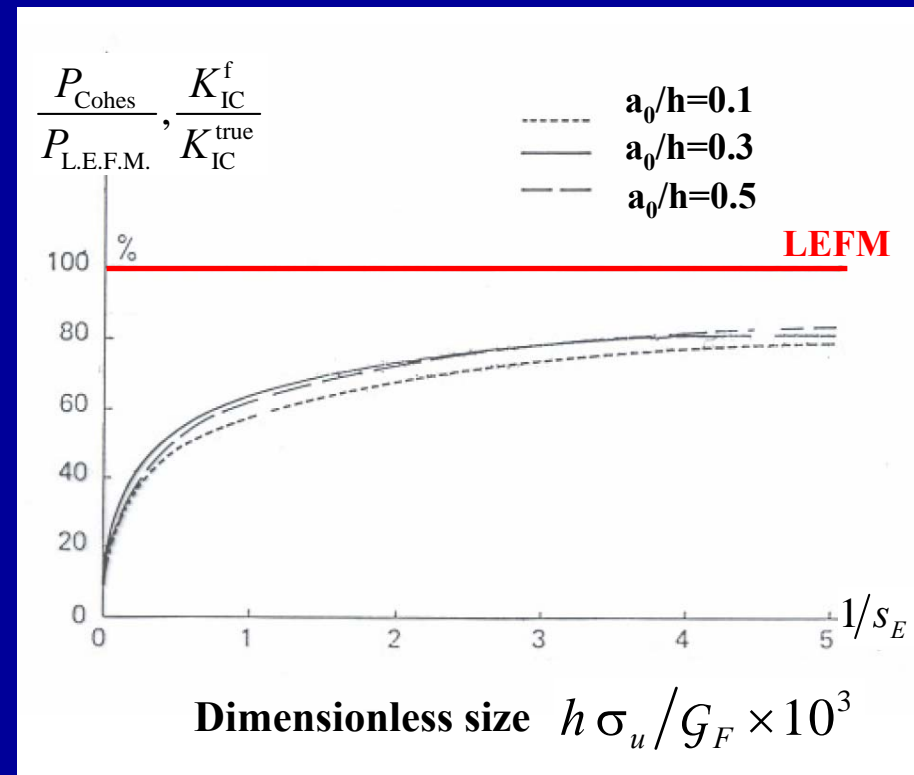
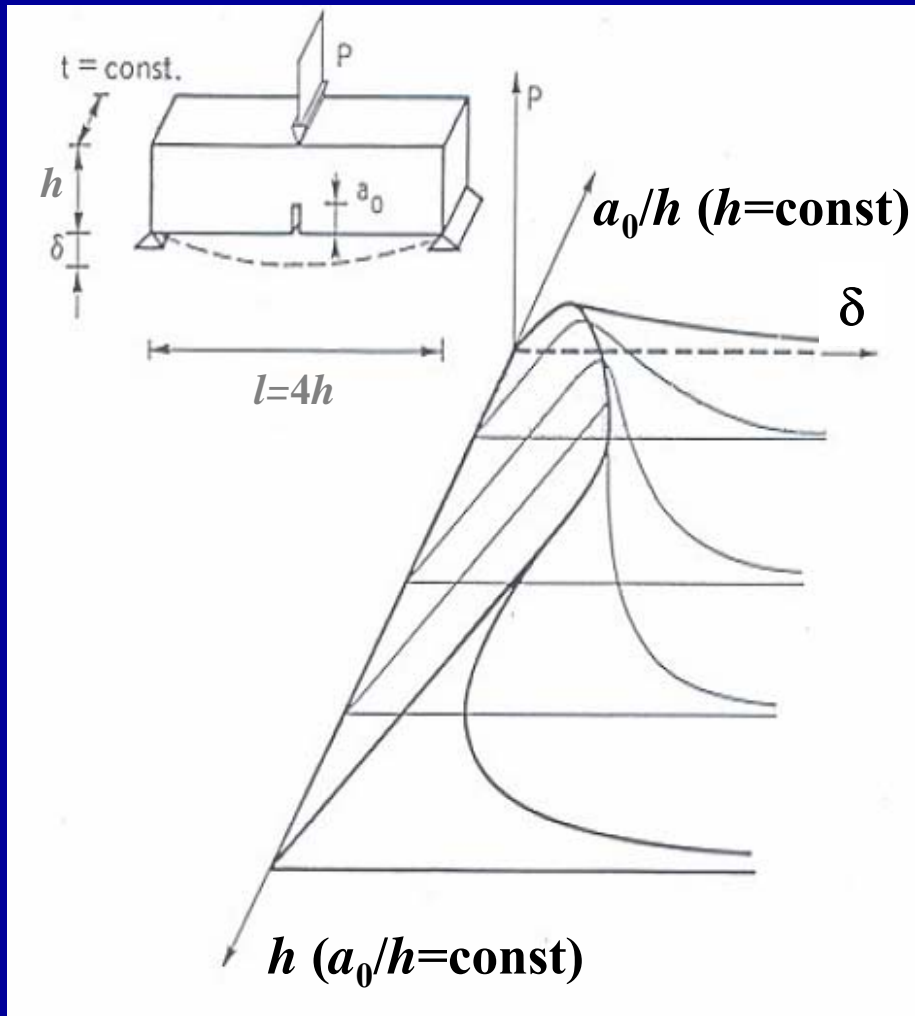
$$\sigma_u t \frac{h^2}{4}$$

$$M_u = M_{\max} / 3$$



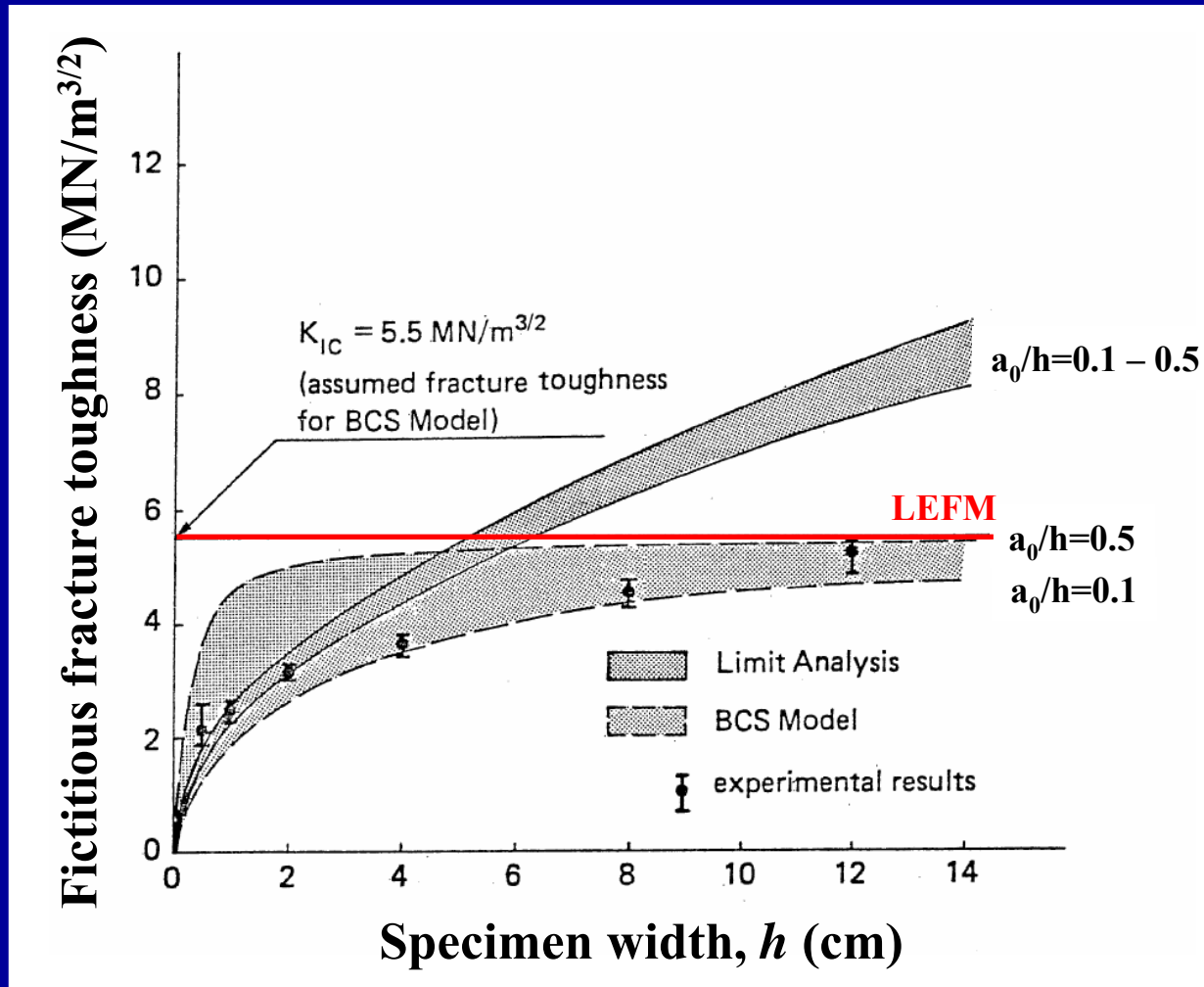
$$\sigma_u t \frac{h^2}{6}$$

Size-scale transition towards LEFM



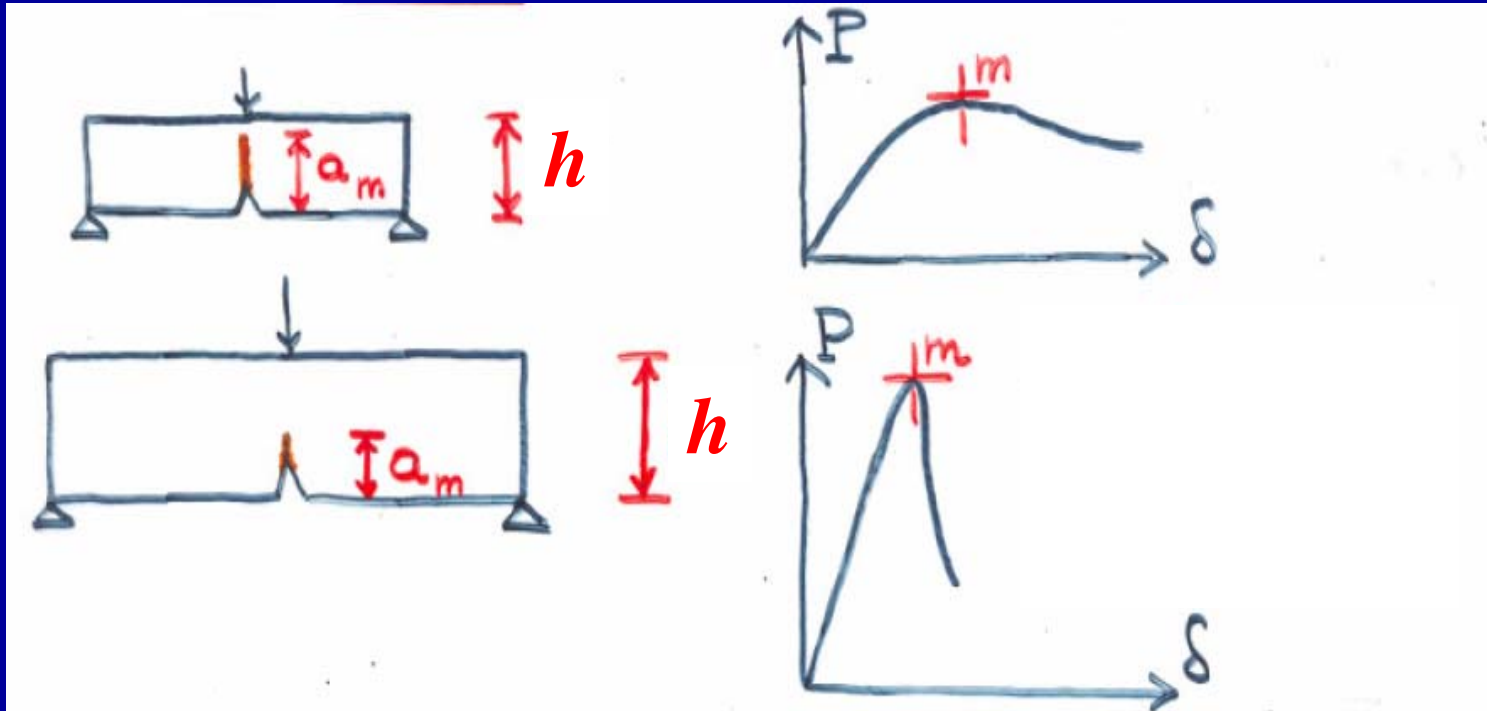
Catastrophe manifold

Comparison with the BCS cohesive model



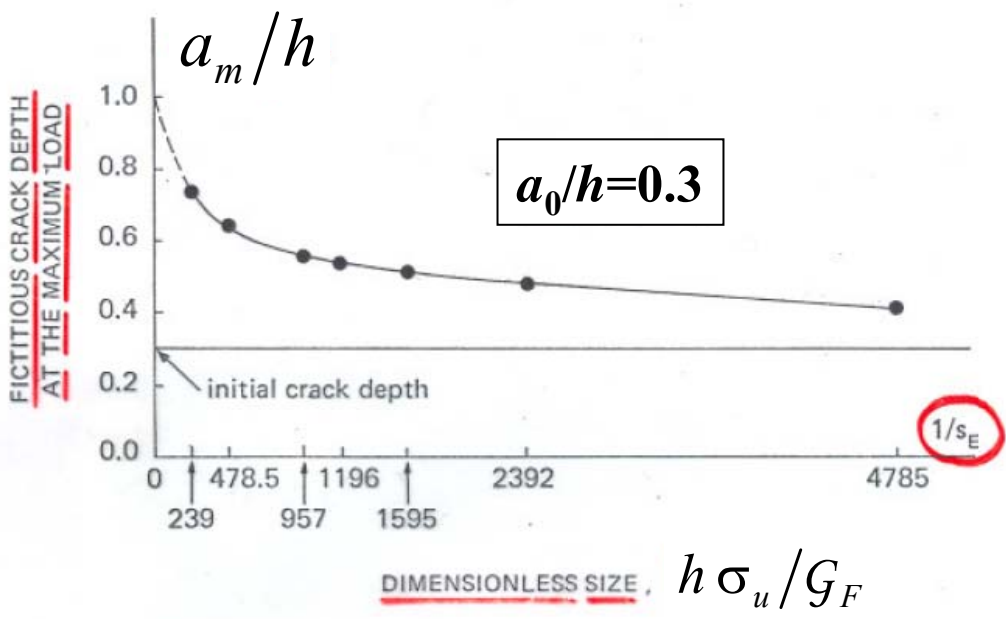
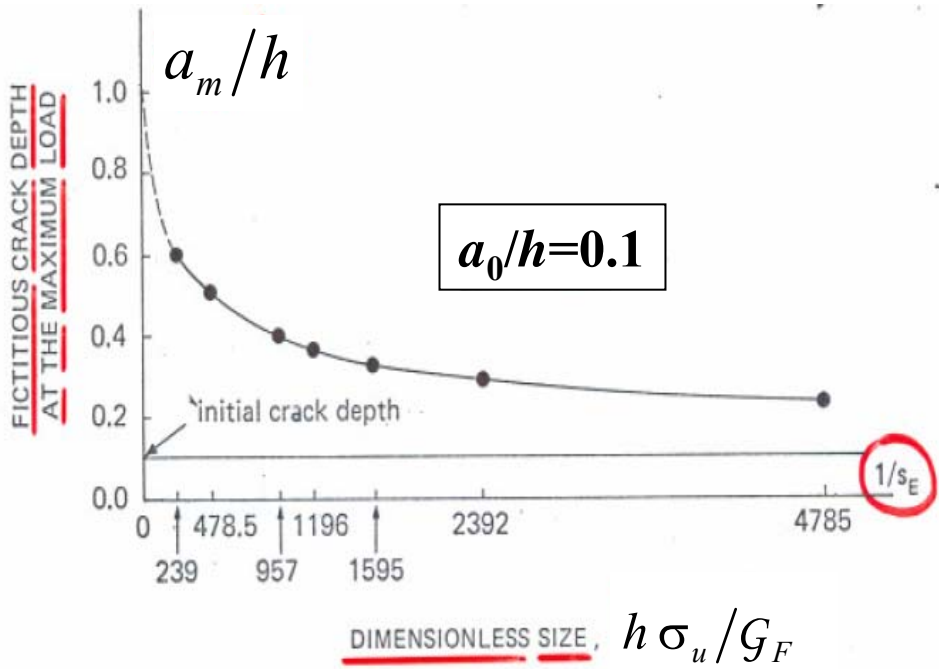
Carpinteri A. (1986) Cohesive crack tip modelling of plastic fracture, in *Fracture Control of Engineering Structures* (Proc. 6th European Conf. on Fracture, 1986), Eds. H.C. van Elst, A. Bakker, EMAS, Sheffield, 75-82.

Fictitious crack depth at the maximum load (a_m/b)

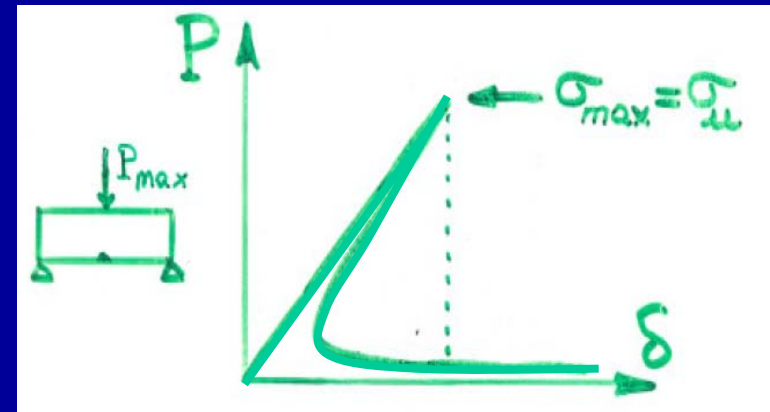
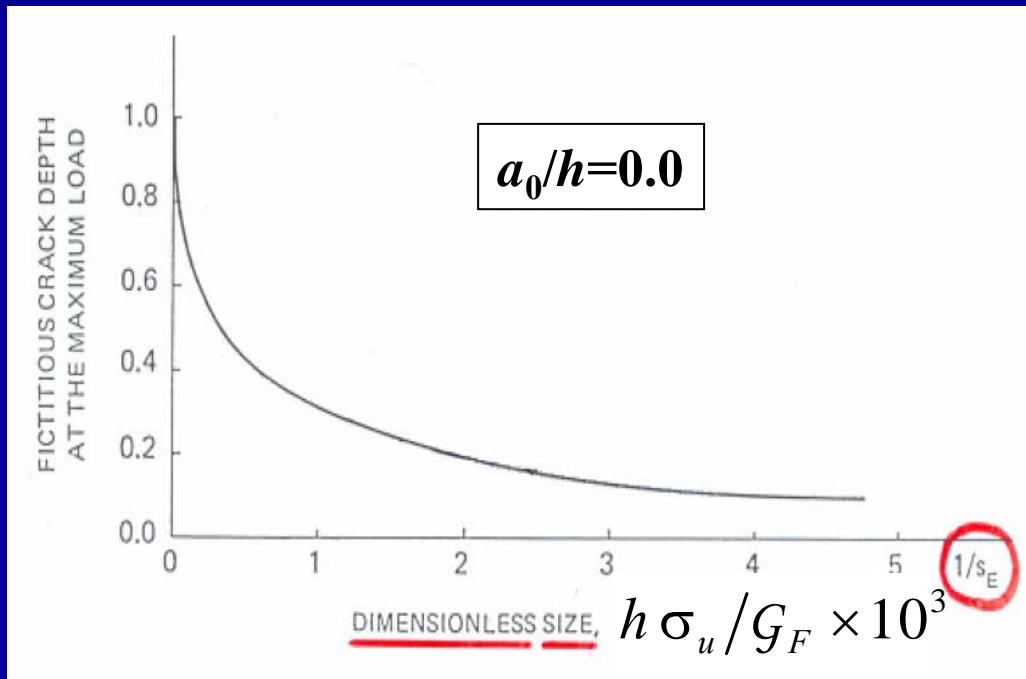


$$S_E = \frac{G_F}{\sigma_u h} \rightarrow 0$$

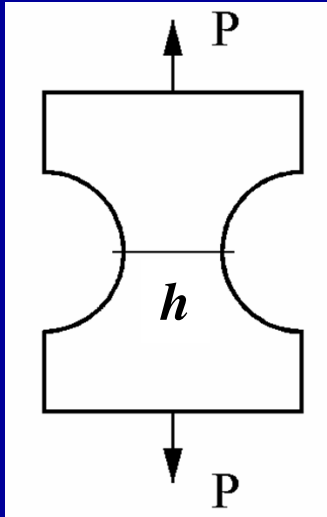
$$a_m \rightarrow a_0 (!)$$



Size-scale transition towards ultimate strength collapse



$$s_E = \frac{G_F}{\sigma_u h} \rightarrow 0$$

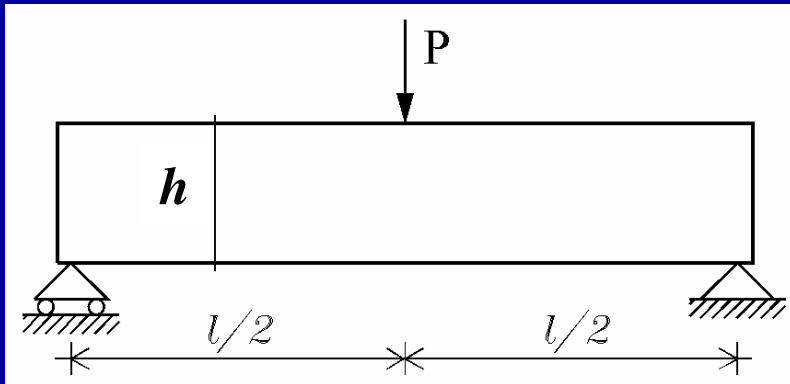


The nominal tensile strength, f_t , can be evaluated by means of the uniaxial tensile test:

$$f_t = \frac{P_u}{th}$$

P_u = maximum load, t = thickness of the specimen.

A scale-dependent value of the tensile strength, σ_u , is obtained by a three-point bending test, using the following expression:



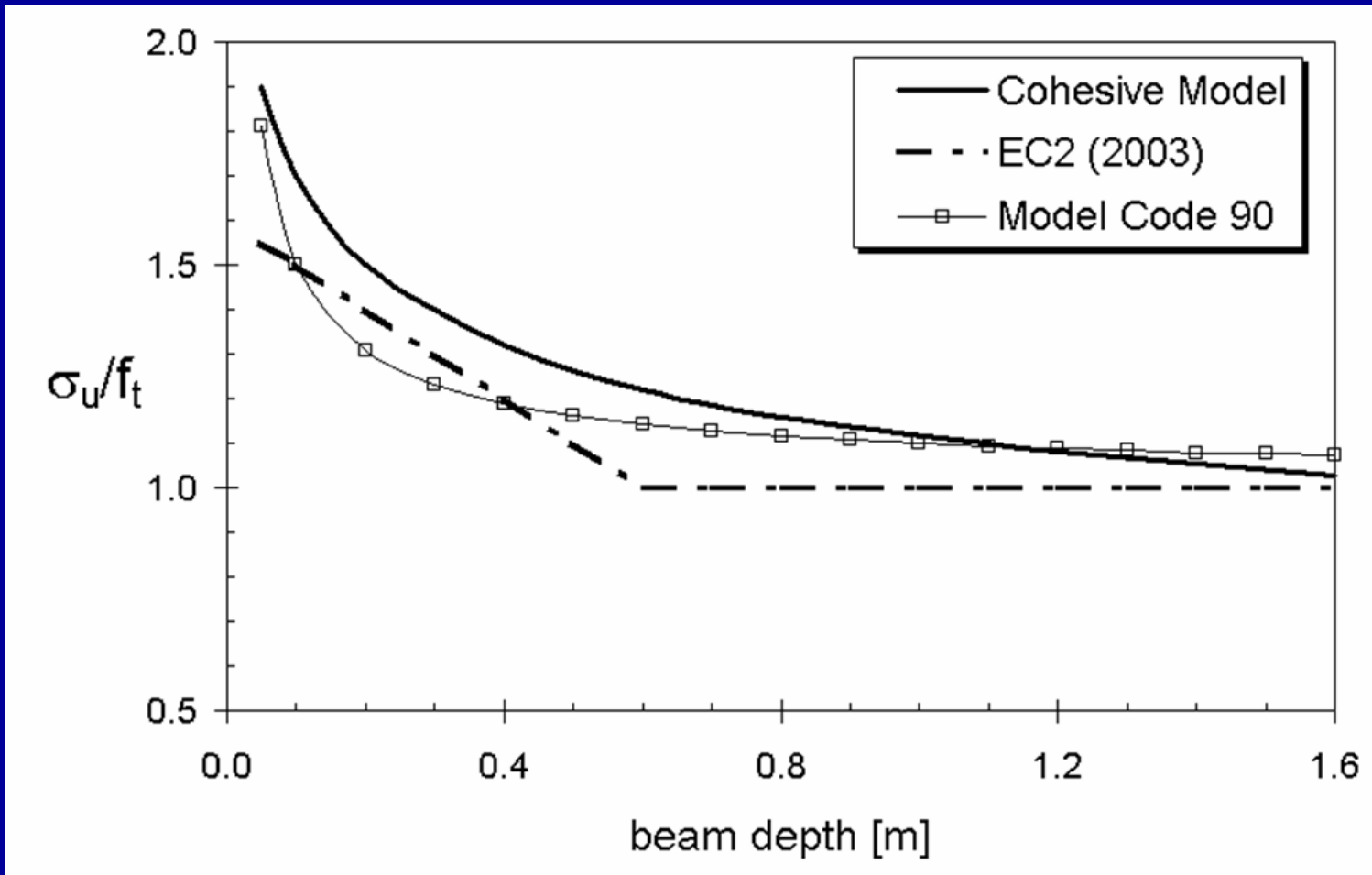
$$\sigma_u = \frac{6M_u}{th^2}$$

where:

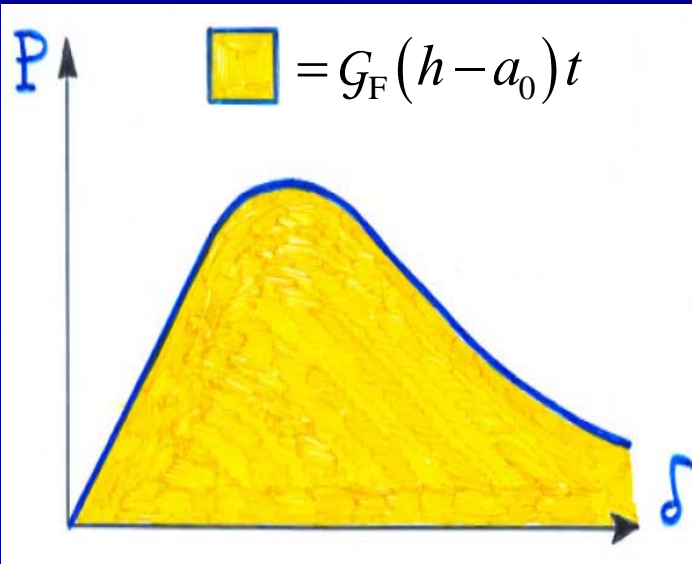
M_u = maximum bending moment in the middle cross section,

t = thickness of the beam.

Comparison with design codes



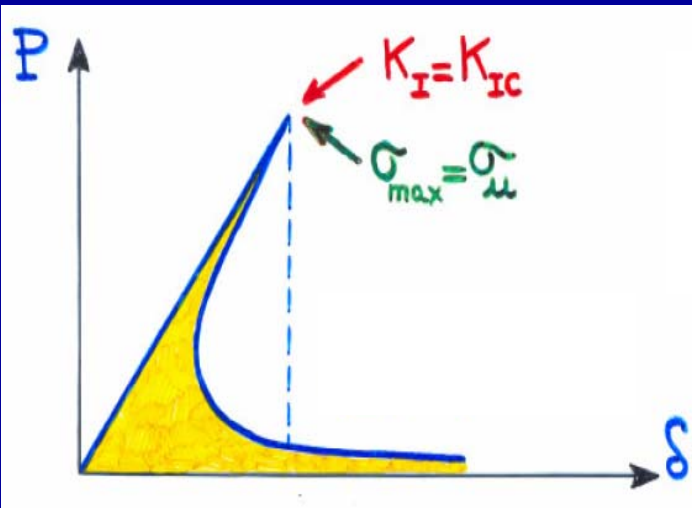
The role of the brittleness number



- high fracture energy G_F
- low tensile strength σ_u
- small size h

$$S_E = \frac{G_F}{\sigma_u h} \nearrow$$

- large initial crack depth a_0/h
- low slenderness l/h

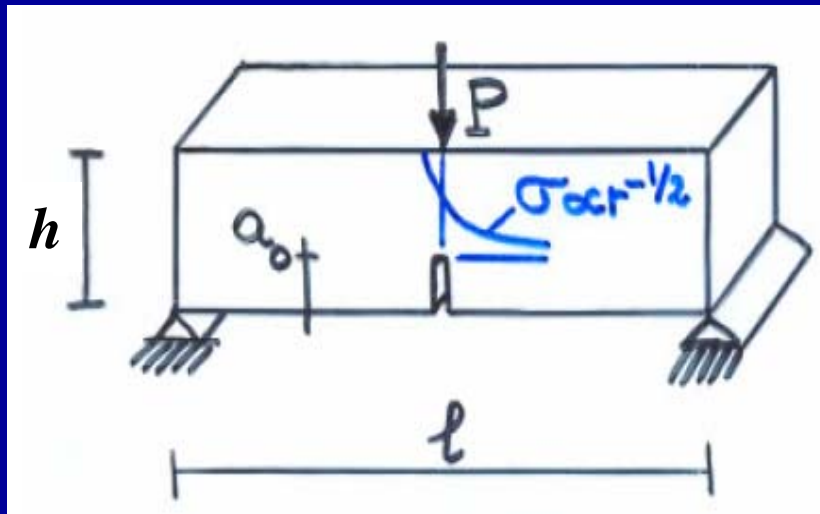


- low fracture energy G_F
- high tensile strength σ_u
- large size h

$$S_E = \frac{G_F}{\sigma_u h} \searrow$$

- small initial crack depth a_0/h
- high slenderness l/h

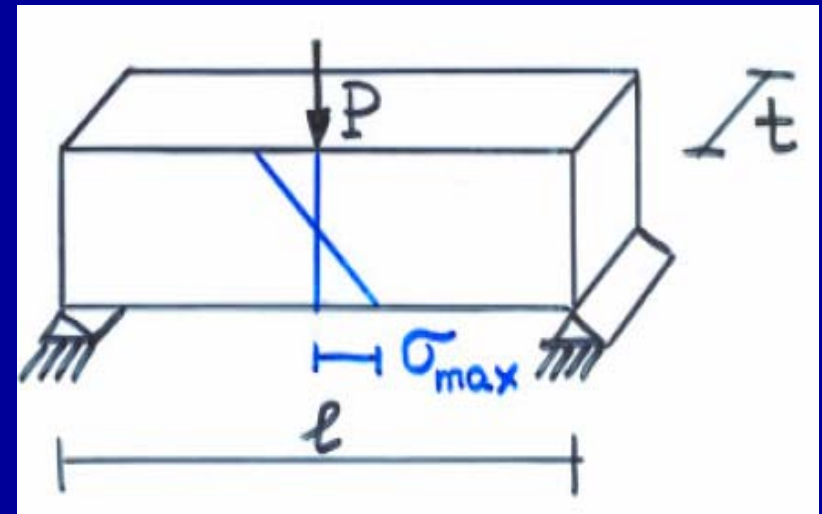
INITIALLY CRACKED



$$K_I = K_{IC}$$

(stress-singularity)

INITIALLY UNCRACKED



$$\sigma_{max} = \sigma_u$$

(Navier stress-distribution)

$$s = \frac{K_{IC}}{\sigma_u \sqrt{h}}$$

Brittleness number (STRESS)

$$s_E = \frac{G_F}{\sigma_u h}$$

Brittleness number (ENERGY)

$$G_F = \frac{K_{IC}^2}{E}$$

Irwin's relationship

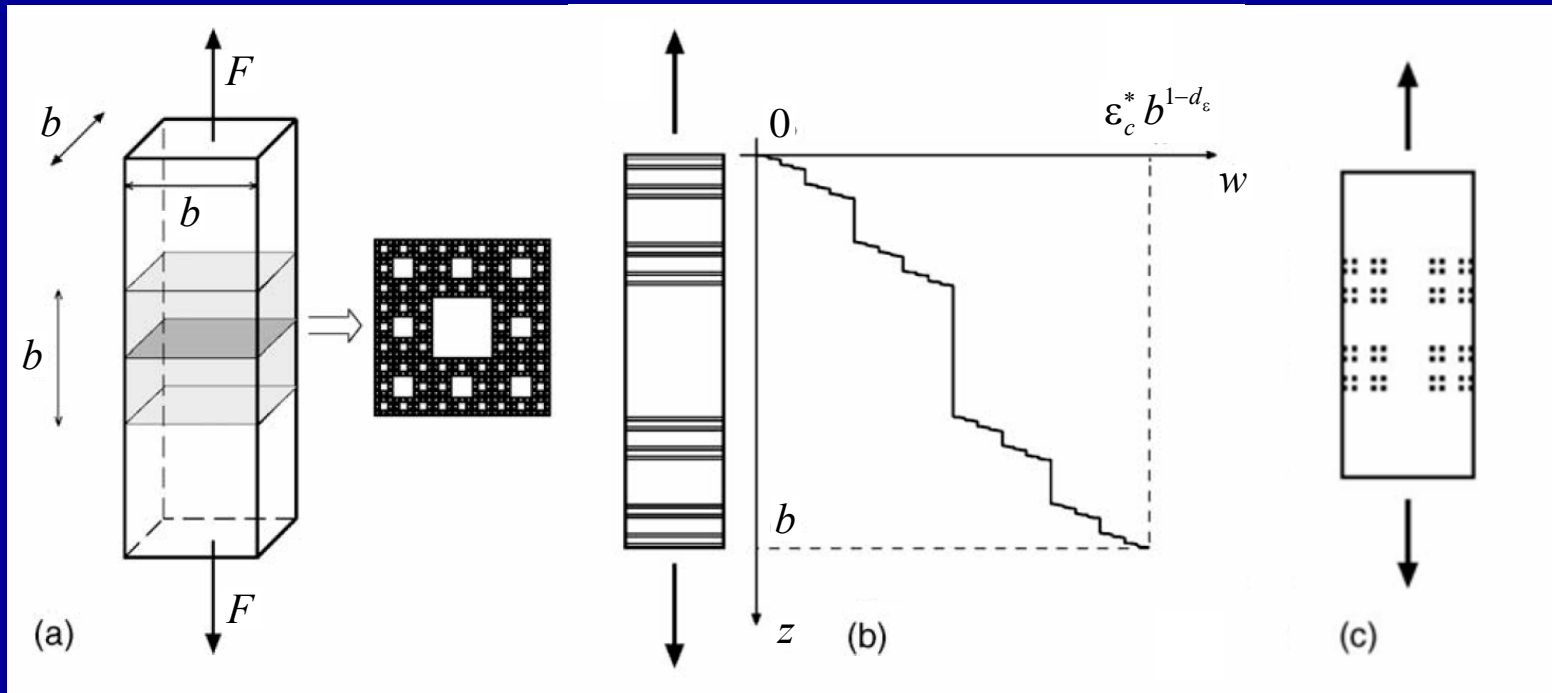


$$s_E = s^2 \varepsilon_u$$

Relationship between s and s_E

Carpinteri A. (1986) Limit analysis for elastic-softening structures: Scale and slenderness influence on the global brittleness, in *Structure and Crack Propagation in Brittle Matrix Composite Materials* (Proc. Euromech Colloquium 204, Warsaw, Poland, 1985), Eds. A.M. Brandt, I.H. Marshall, Elsevier Applied Science, London, 497-508.

Fractal Cohesive Crack Model



Resistant cross-section: lacunar fractal of dimension $D=2-d_\sigma$

Deformation bands: lacunar fractal of dimension $D=1-d_\epsilon$

Damage domain: invasive fractal of dimension $D=2+d_G$

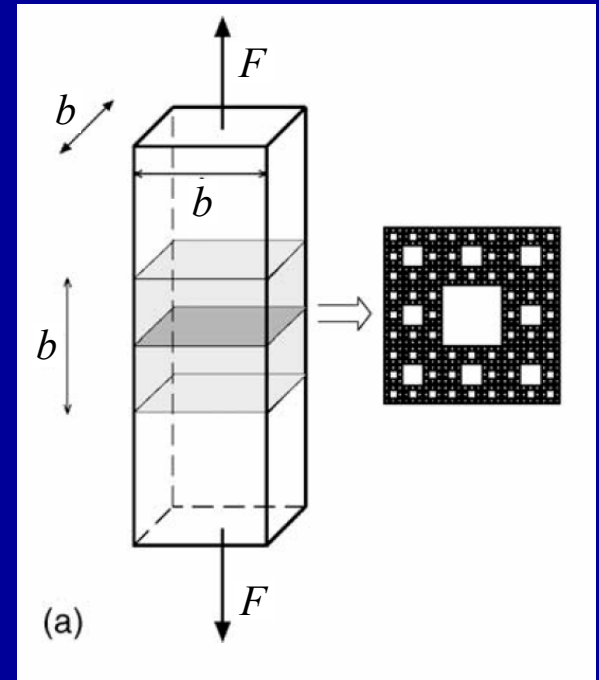
- These three fractal domains are the cause of the size-scale effects on the nominal values of tensile strength σ_u , critical deformation ϵ_c and fracture energy G_F (Carpinteri, 1994).

- **By renormalizing:**

$$F = \sigma_u A_0 = \sigma_u^* A_{res}^*$$

where: $A_0 = b^2$, $A_{res}^* = b^{(2-d_\sigma)}$.

- **The fractal tensile strength σ_u^* is the true scale-invariant material constant and presents fractal physical dimensions: $\sigma_u = \sigma_u^* b^{-d_\sigma}$.**

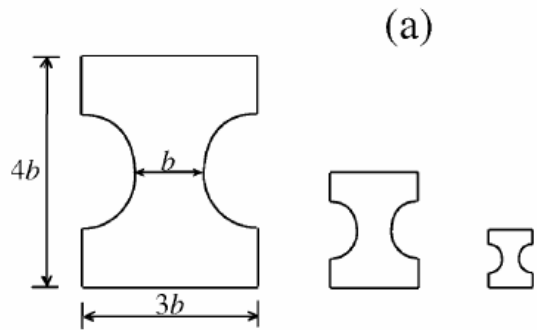


- **Analogous reasoning gives, for critical deformation ε_c and fracture energy G_F respectively:**

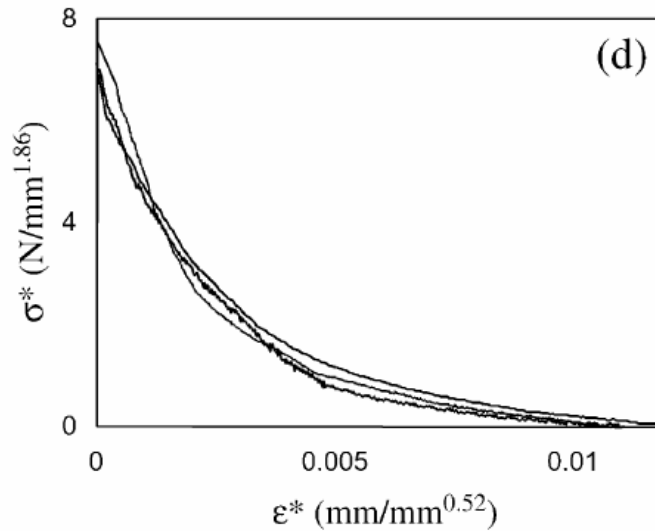
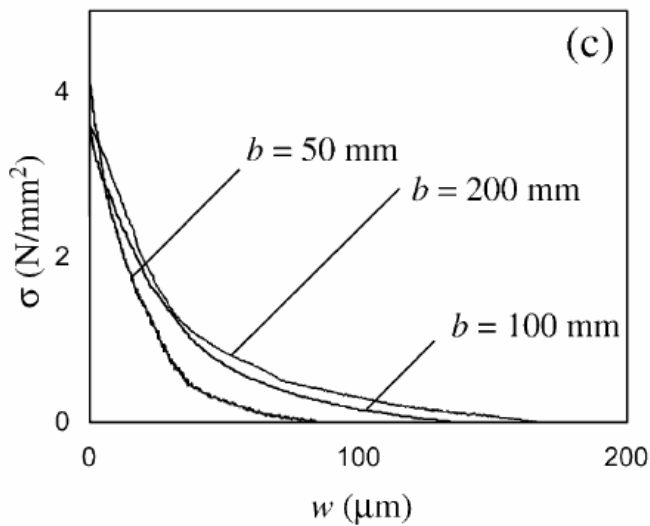
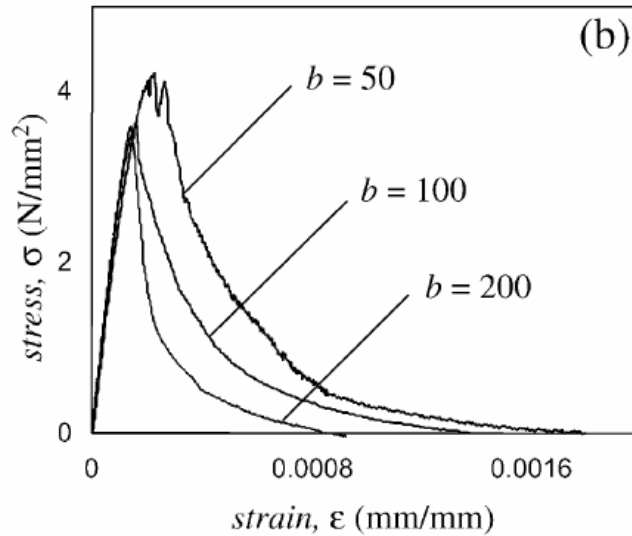
$$\varepsilon_c = \varepsilon_c^* b^{-d_\varepsilon} \quad G_F = G_F^* b^{d_G}$$

- **The three power-law exponents are not independent:**

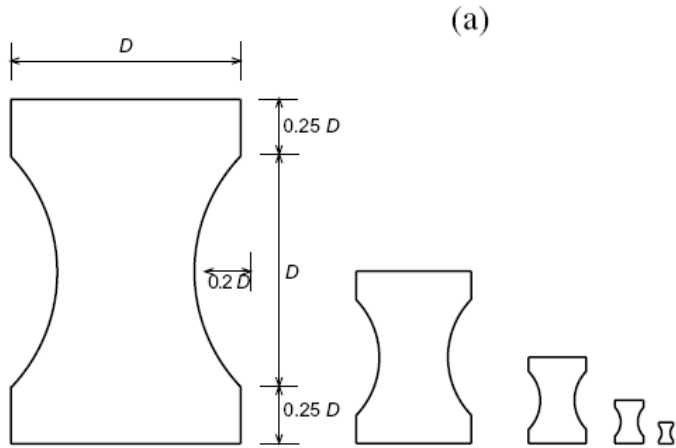
$$d_\sigma + d_\varepsilon + d_G = 1$$



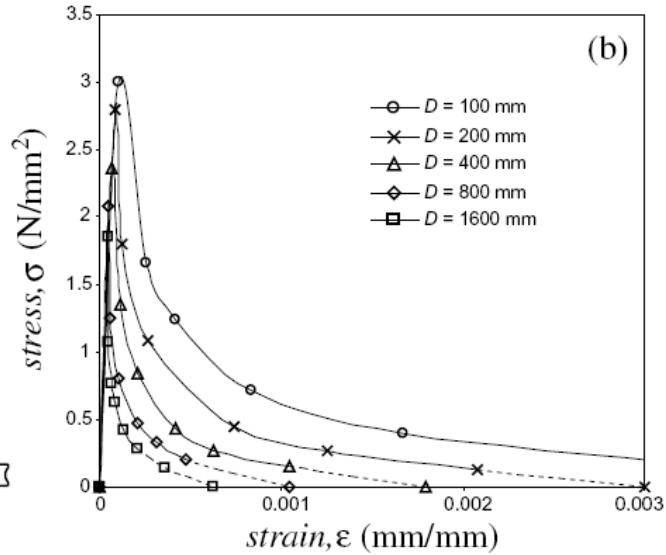
Carpinteri and Ferro, 1994



The three size-dependent curves collapse onto a unique one!

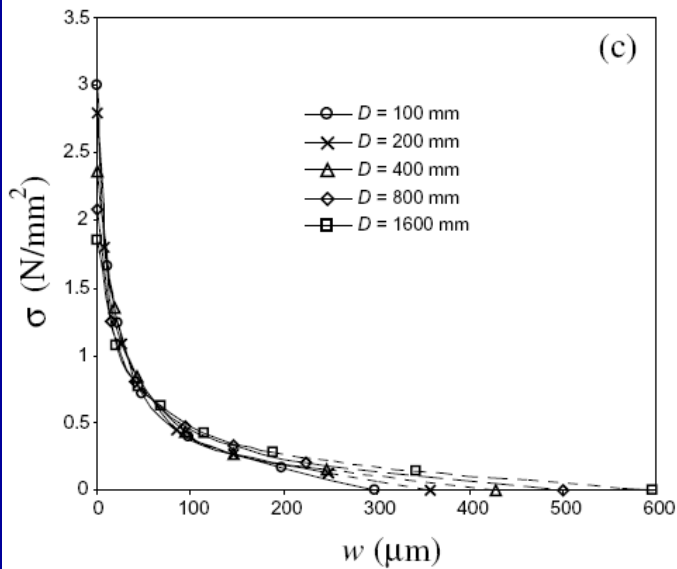


(a)

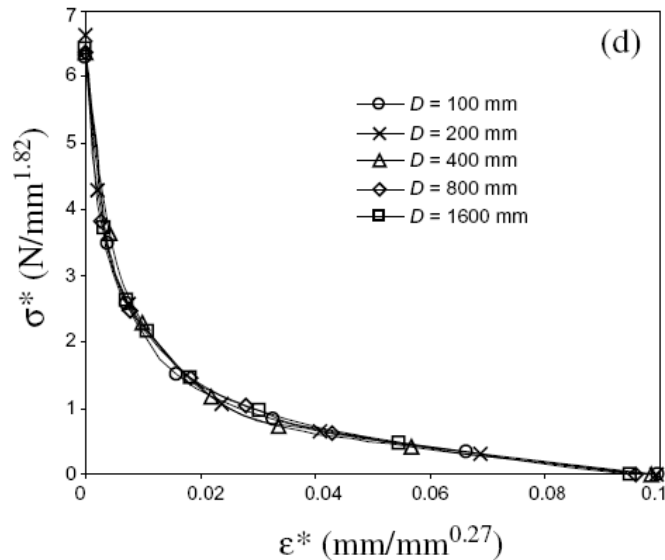


(b)

Van Mier and van Vliet, 1999



(c)

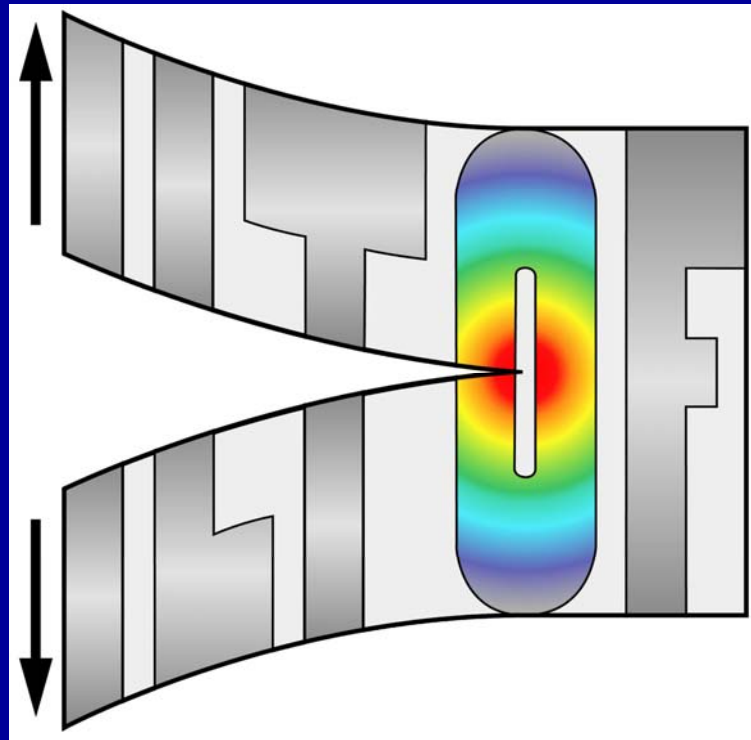


(d)

The five size-dependent curves collapse onto a unique one!

Acknowledgements

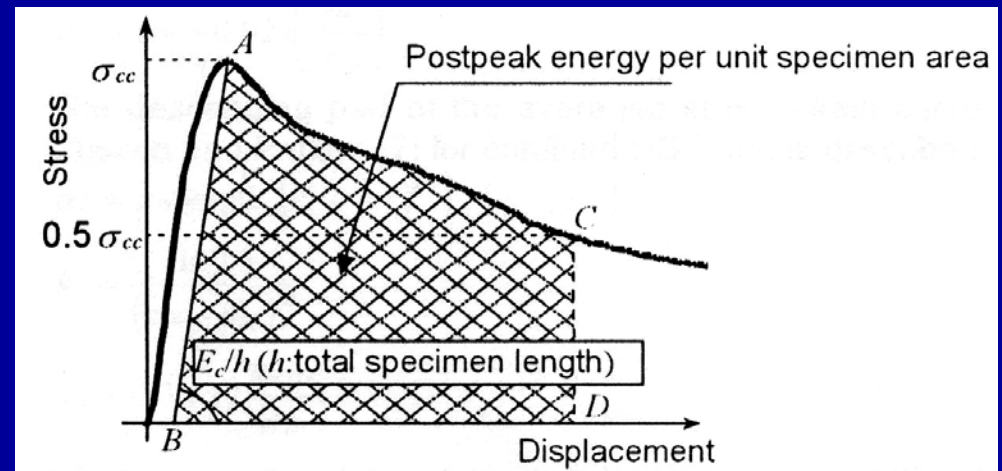
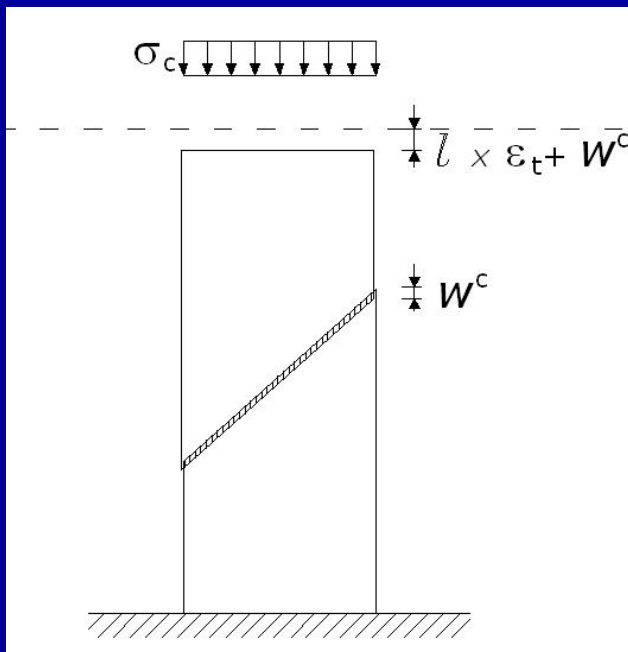
The financial support of the European Union to the project “*Innovative Learning and Training On Fracture (ILTOF)*” is gratefully acknowledged.



Overlapping crack model

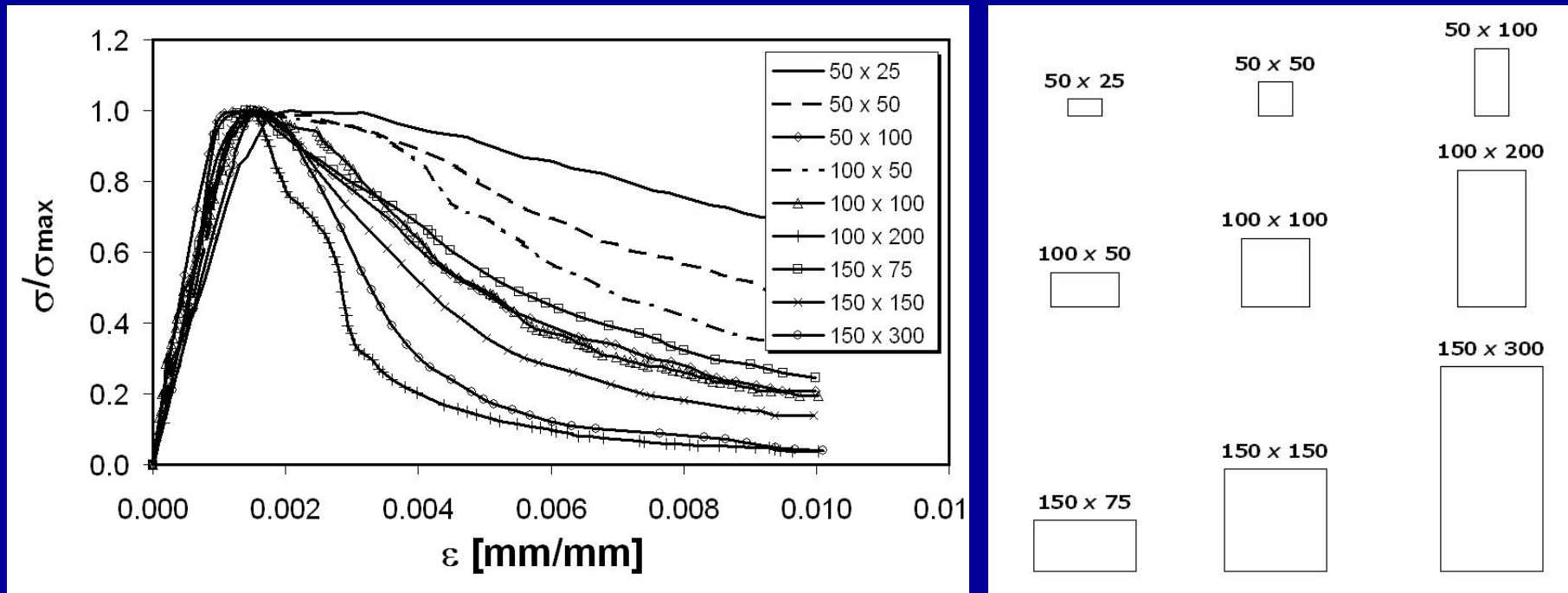
Quasi-brittle materials show the phenomenon of strain localization in compression when the elastic limit is overcome.

We can define a *crushing energy* (per unit surface), as the area below the softening curve in the $\sigma - w$ diagram.

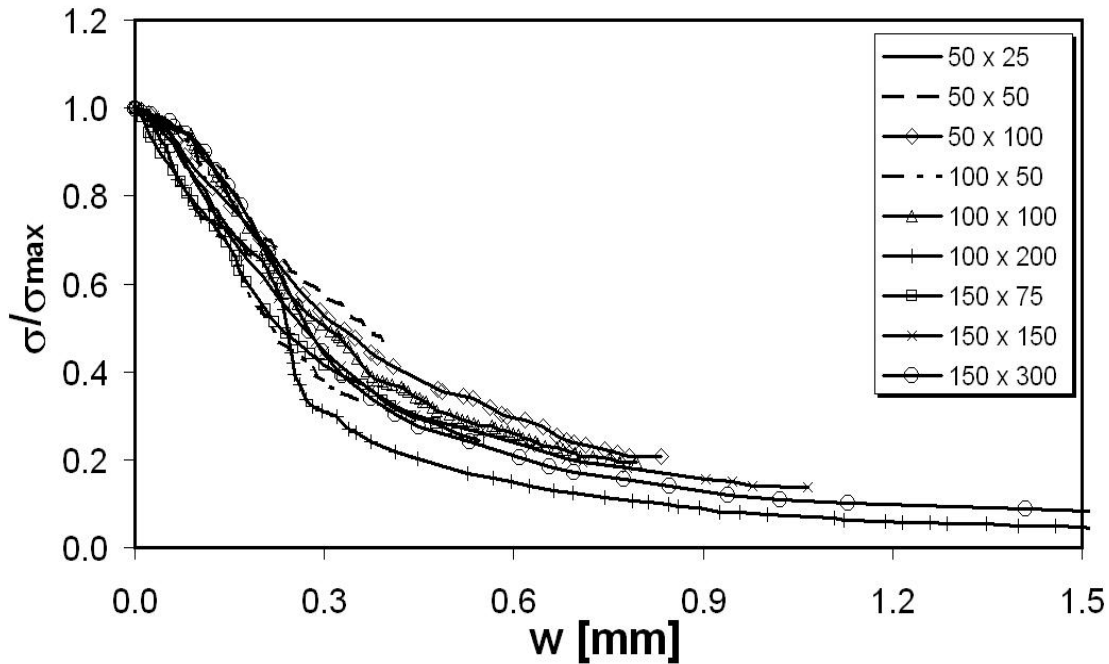
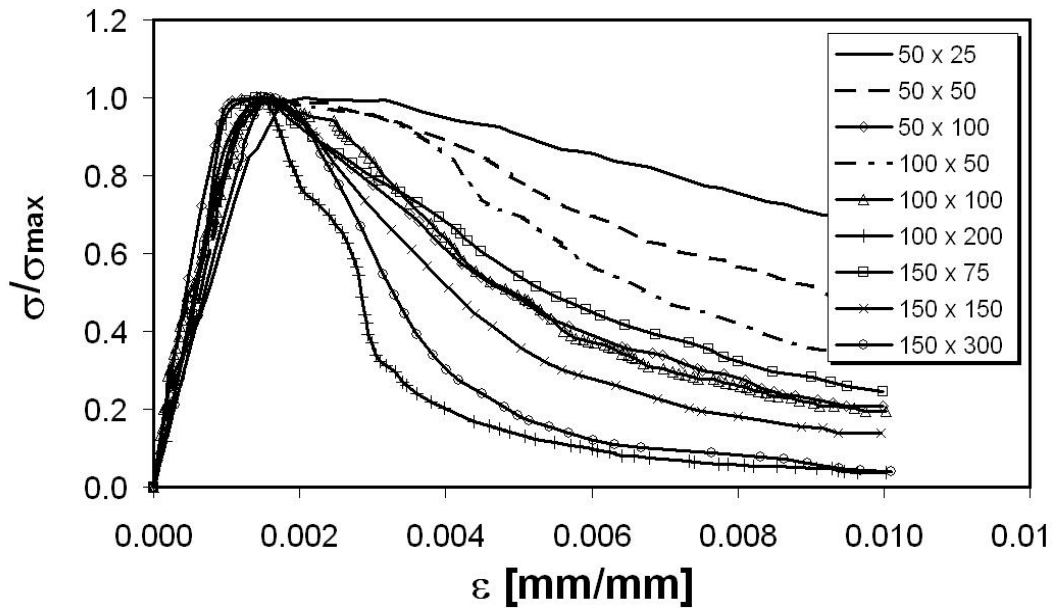


Van Mier 1984; Dahl e Brincker 1989; Van Vliet e Van Mier 1996;
Jansen e Shah 1997; Suzuki et al. 2006.

The crushing energy is a *true material parameter*, as can be demonstrated from the application to uniaxial compressive tests of concrete specimens with different slenderness and/or size-scale.

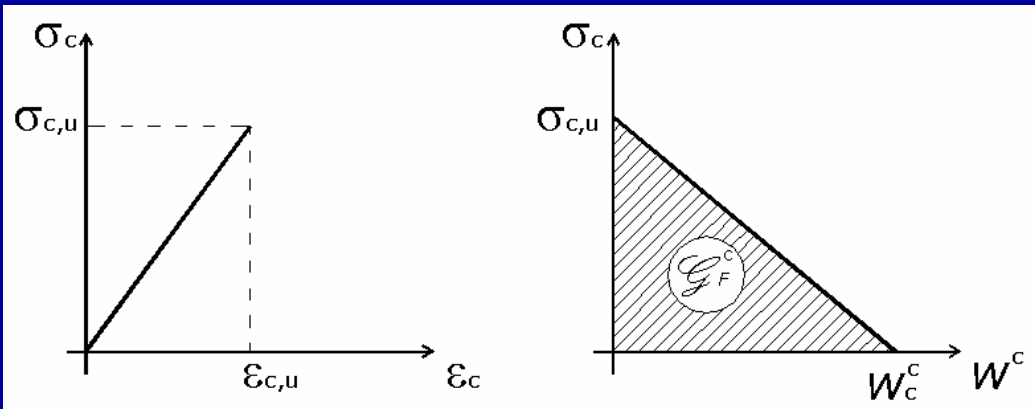
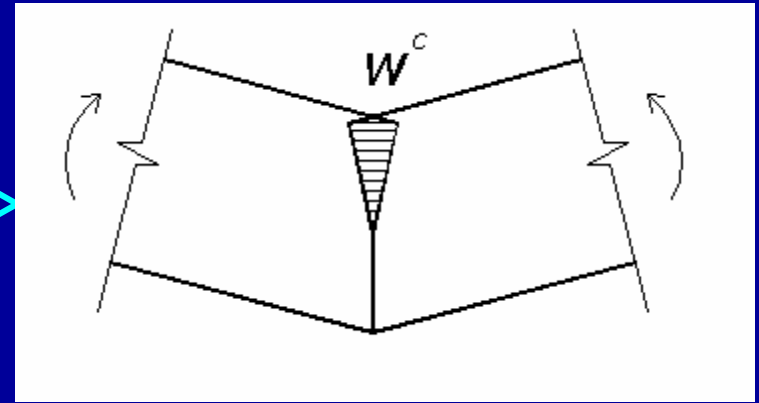
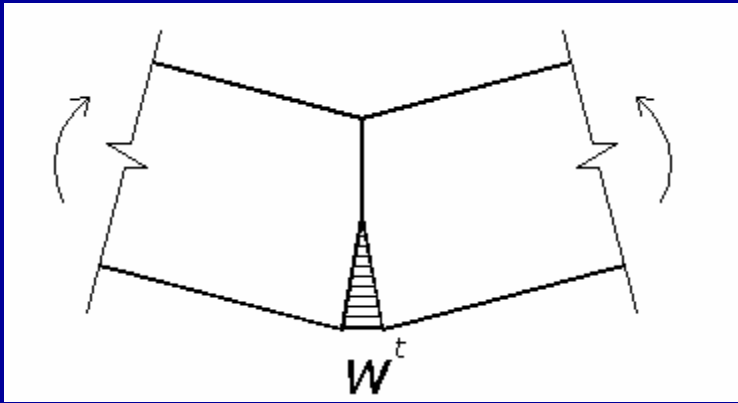


(Ferrara and Gobbi, 1995)



The slenderness- and scale-dependent curves collapse onto a narrow band!

In analogy with the *Cohesive Crack Model*, the *Overlapping Crack Model* can be defined by a couple of constitutive laws:



$$G_F^c = 30 \div 60 \text{ N/mm}$$

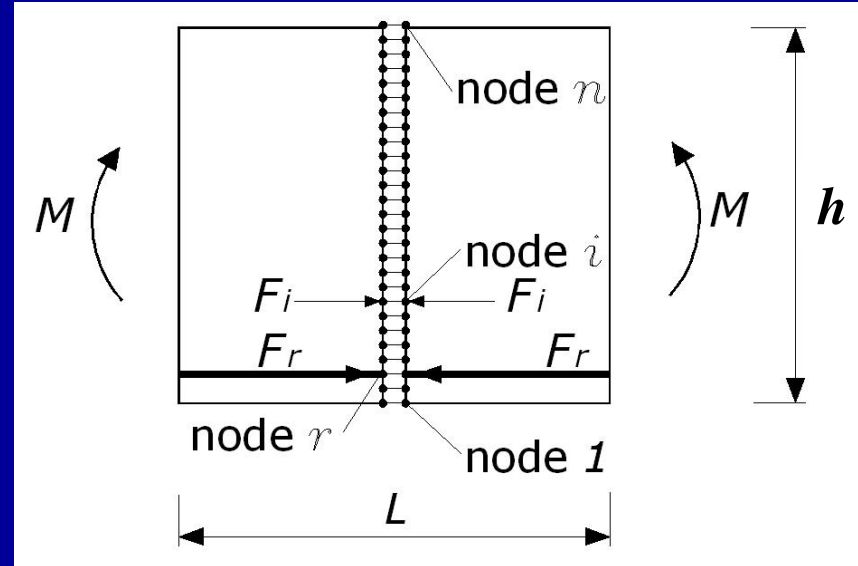
$$w_c^c \cong 1 \text{ mm}$$

Carpinteri A., Corrado M., Paggi M., Mancini G. (2007) Cohesive versus overlapping crack model for a size effect analysis of RC elements in bending, In: *Design, Assessment and Retrofitting of RC Structures*, Vol. 2 of FraMCoS-6, Catania, Italy, Taylor & Francis, 655-663.

Numerical algorithm for RC beams in bending

Equation set consisting in n equations:

$$\{F\} = [K_w] \{w\} + \{K_m\} M$$



$\{F\}$ Nodal force vector

$[K_w]$ Stiffness matrix related to the nodal displacements ($w_i = 1$)

$\{w\}$ Horizontal nodal displacements vector

$\{K_m\}$ Influence coefficients vector for the bending moment

M Applied bending moment

$2n+1$ unknowns: $\{F\}$, $\{w\}$ and M

Additional equations:

$$F_i = 0 \quad \text{for } i = 1, 2, \dots, (j-1); \quad i \neq r$$

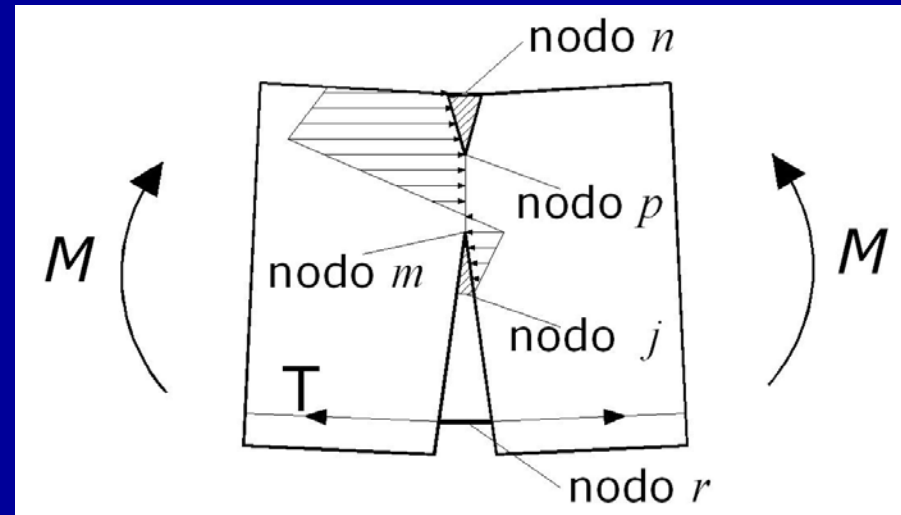
$$F_i = F_{t,u} \left(1 - \frac{w_i^t}{w_c^t} \right) \quad \text{for } i = j, \dots, (m-1)$$

$$w_i^t = 0 \quad \text{for } i = m, \dots, p$$

$$F_i = F_{c,u} \left(1 - \frac{w_i^c}{w_c^c} \right) \quad \text{for } i = (p+1), \dots, n$$

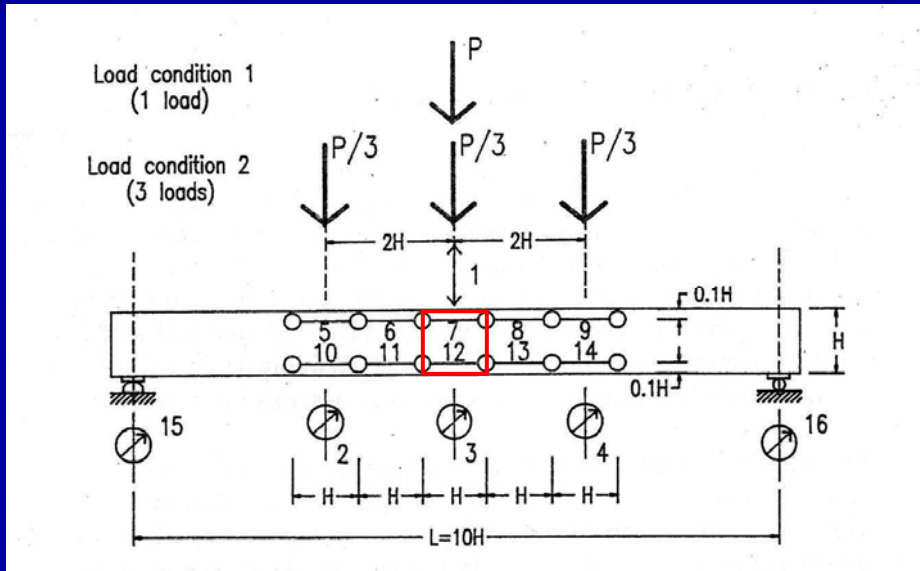
n equations

$$F_m = F_{t,u} \quad \text{or} \quad F_p = F_{c,u}$$



Experimental assessment of the proposed model

Bosco and Debernardi (1992)



GEOMETRY

$$h = 200, 400, 600 \text{ mm}$$

$$L/h = 10$$

$$\rho_t = 0.13\% \div 1.71\%$$

$$\rho_c = 0.12\% \div 0.5\%$$

CONCRETE

$$f_t = 3 \text{ MPa}$$

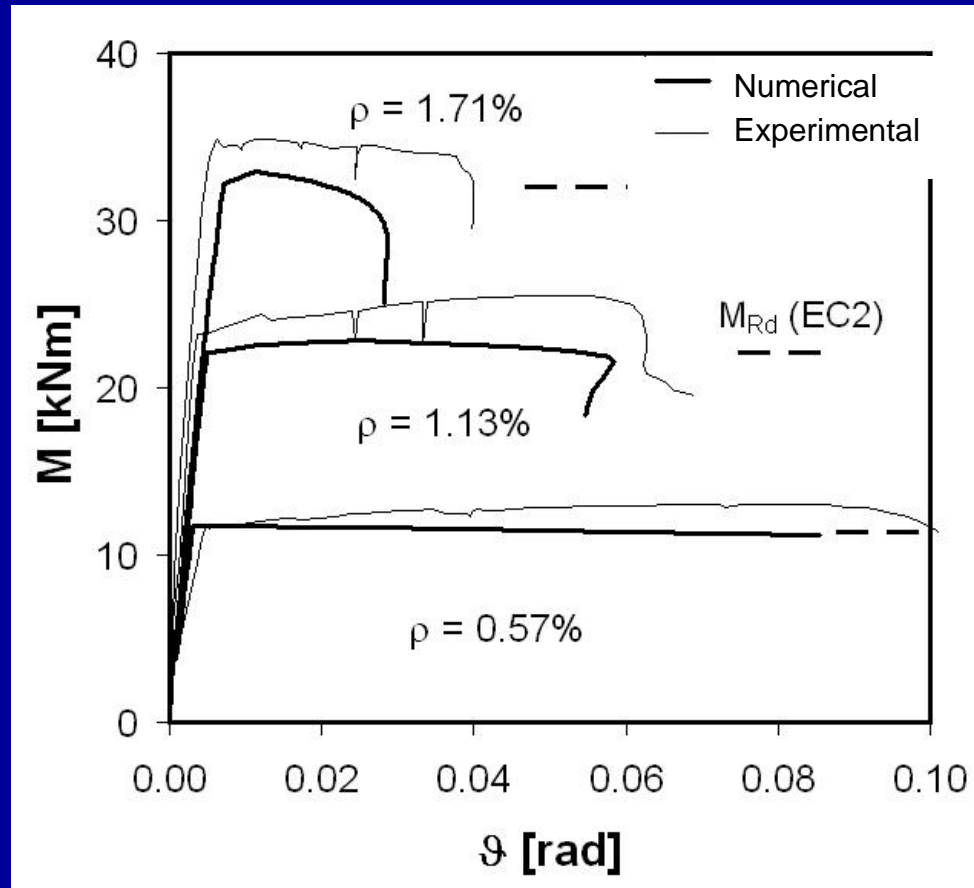
$$f_c = 30 \text{ MPa}$$

$$G_F = 0.065 \text{ N/mm}$$

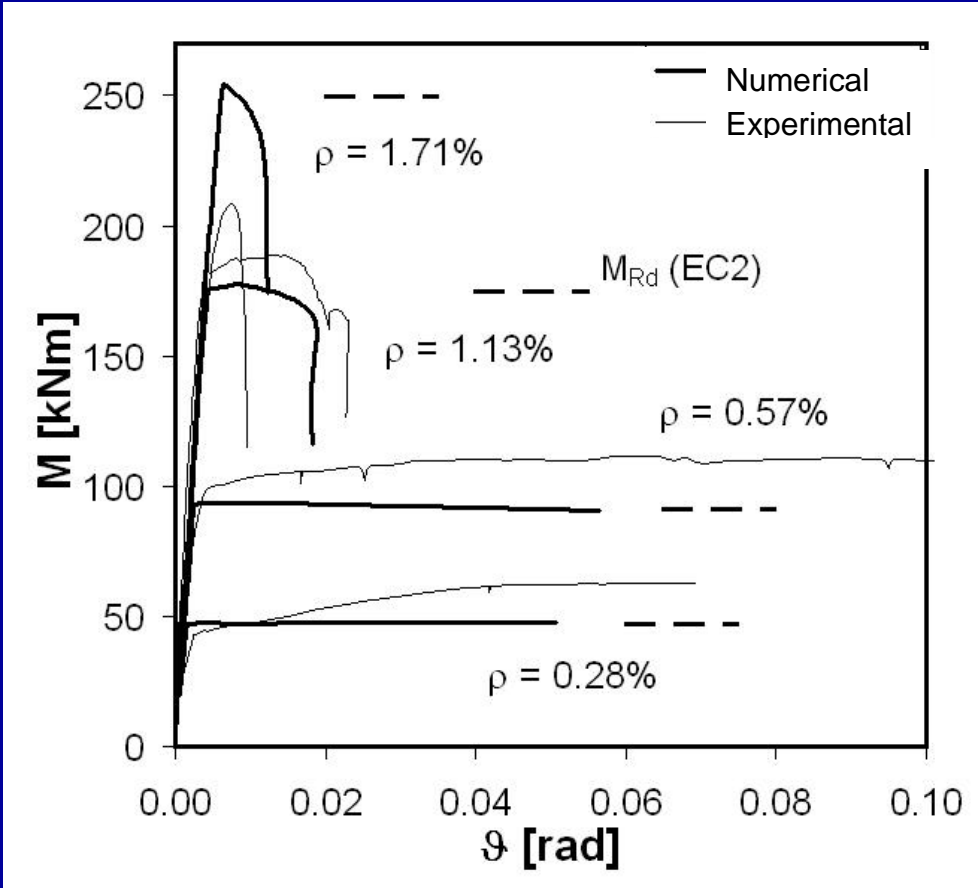
$$G_F^c = 30 \text{ N/mm}$$

Bending moment-rotation diagrams as functions of the reinforcement percentage and of the beam size

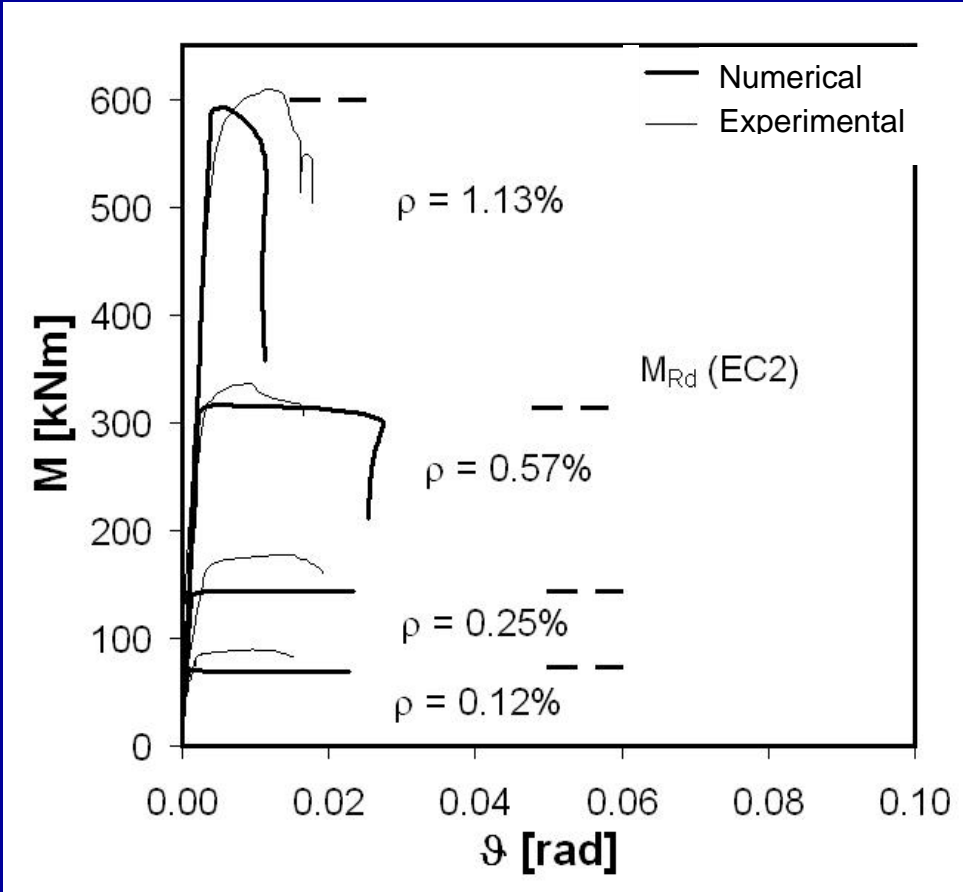
$h = 200 \text{ mm}$



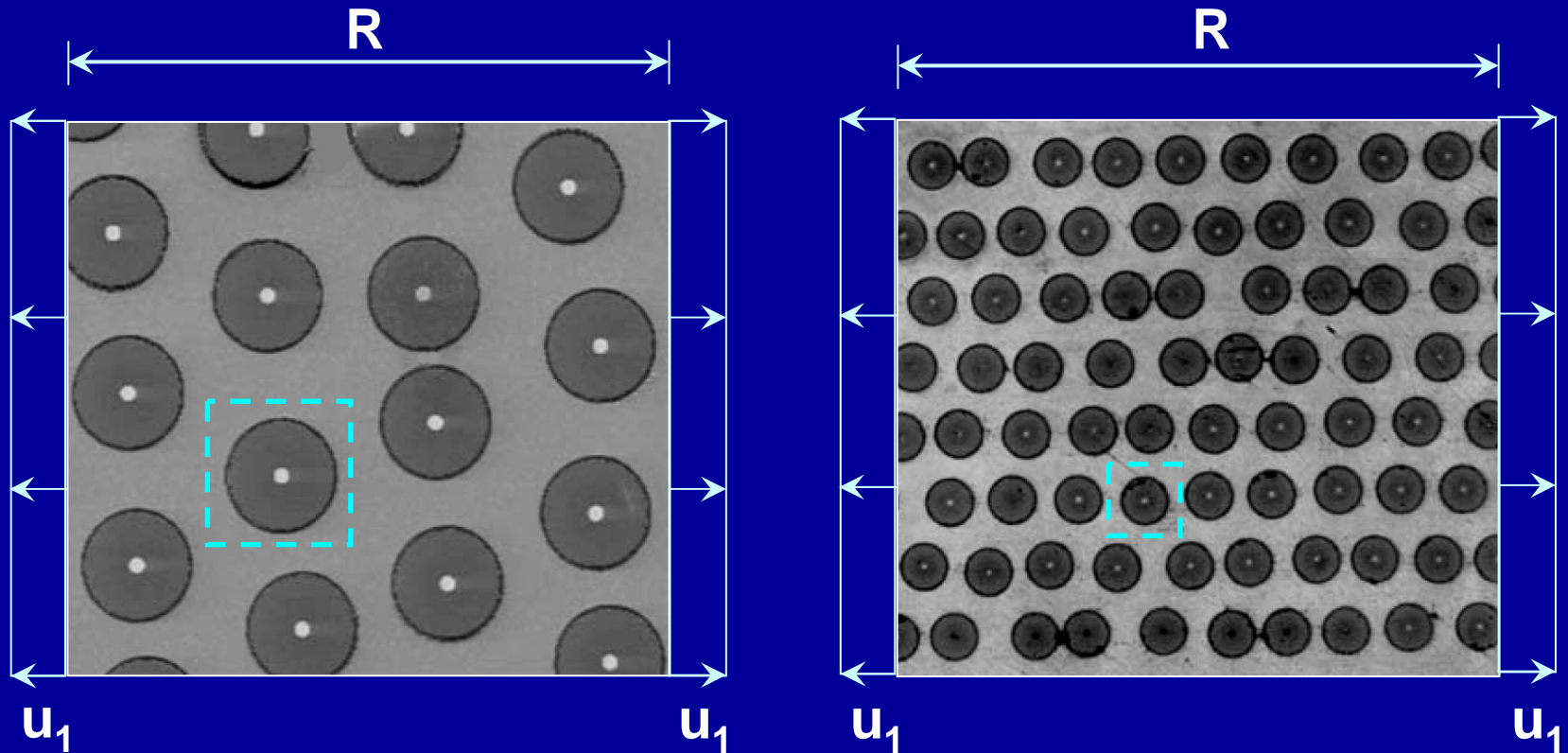
$h = 400 \text{ mm}$



$h = 600 \text{ mm}$



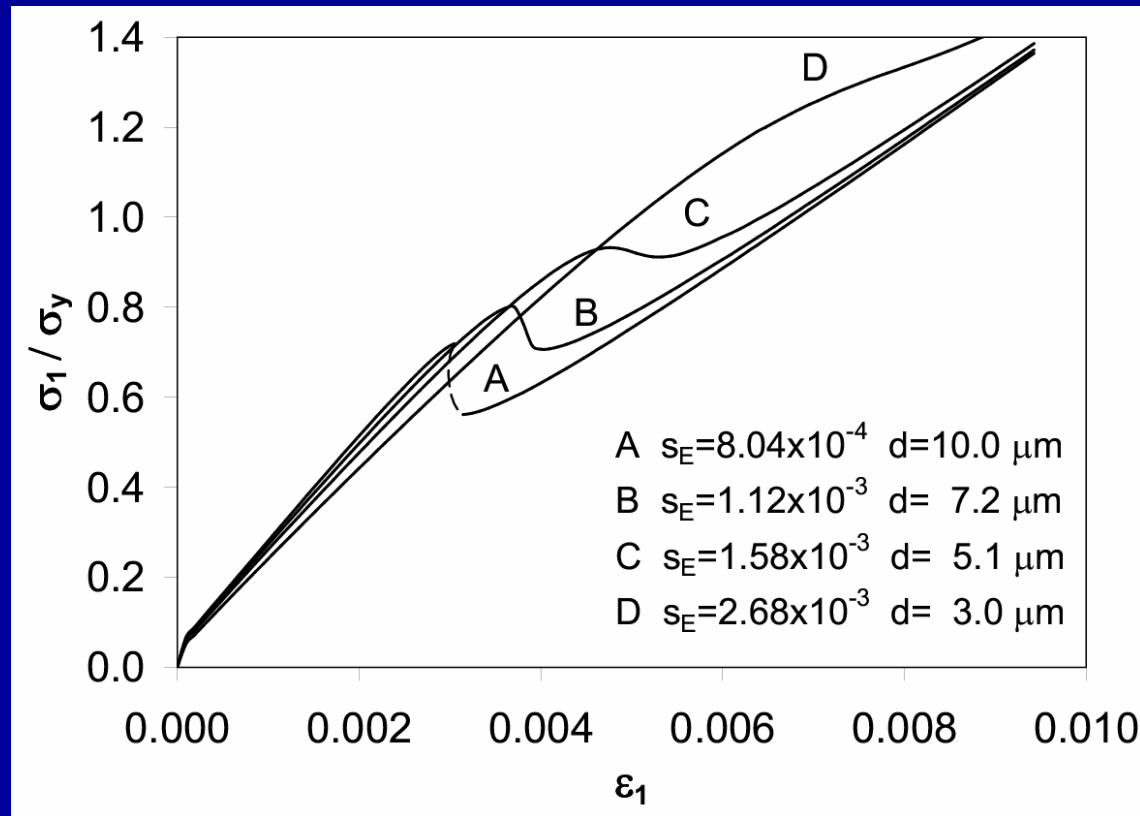
Snap-back instability in micro-structured composites



The macroscopic responses, σ_1 vs. ε_1 , with $v_f = \text{const}$ are compared

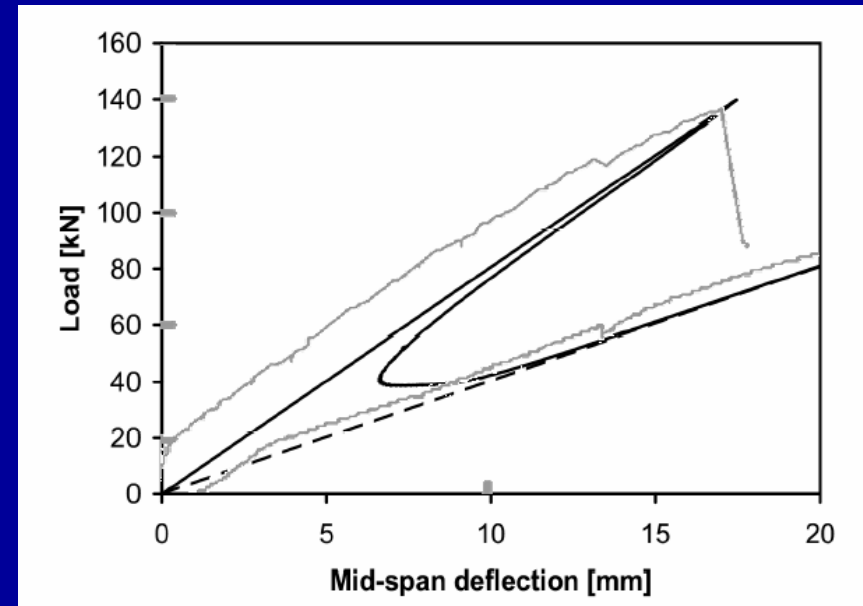
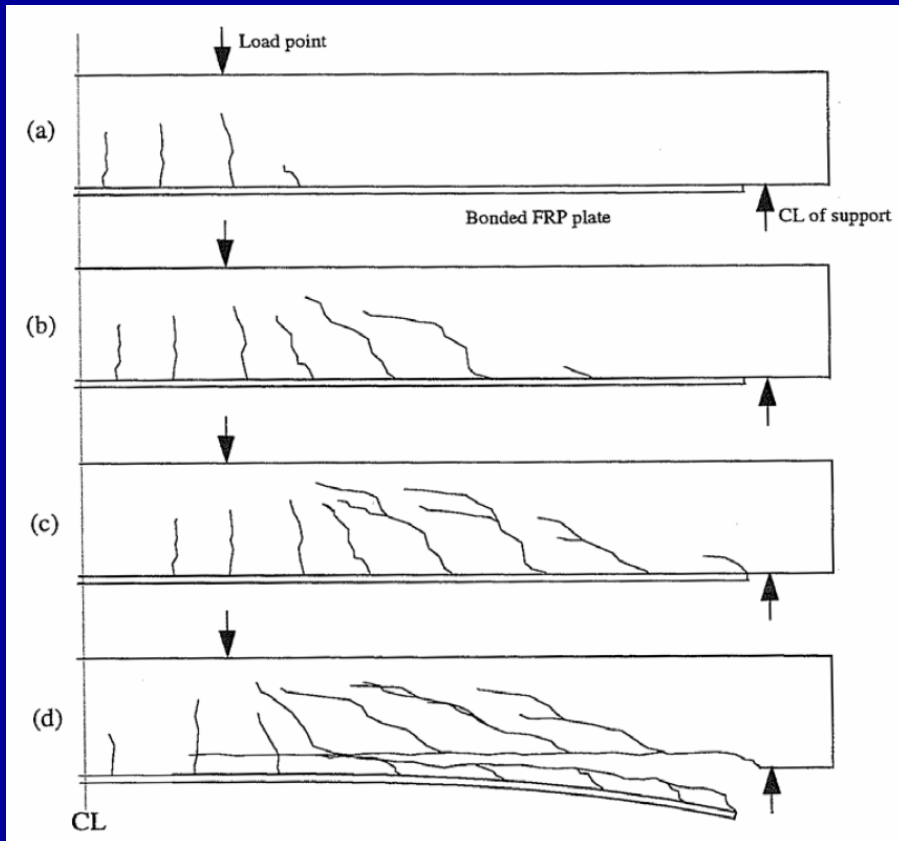
Carpinteri A., Paggi M., Zavarise G. (2005) Snap-back instability in micro-structured composites and its connection with superplasticity, *Strength, Fracture and Complexity*, 3:61-72.

$$\frac{\sigma_1}{\sigma_y} = \Pi \left(\frac{G_{IC}^i}{\sigma_y h}, \varepsilon_1, \frac{\sigma_{\max,0}}{\sigma_y}, \frac{E_f}{E_m}, \frac{V_f}{V_f + V_m}, \nu_f, \nu_m \right)$$



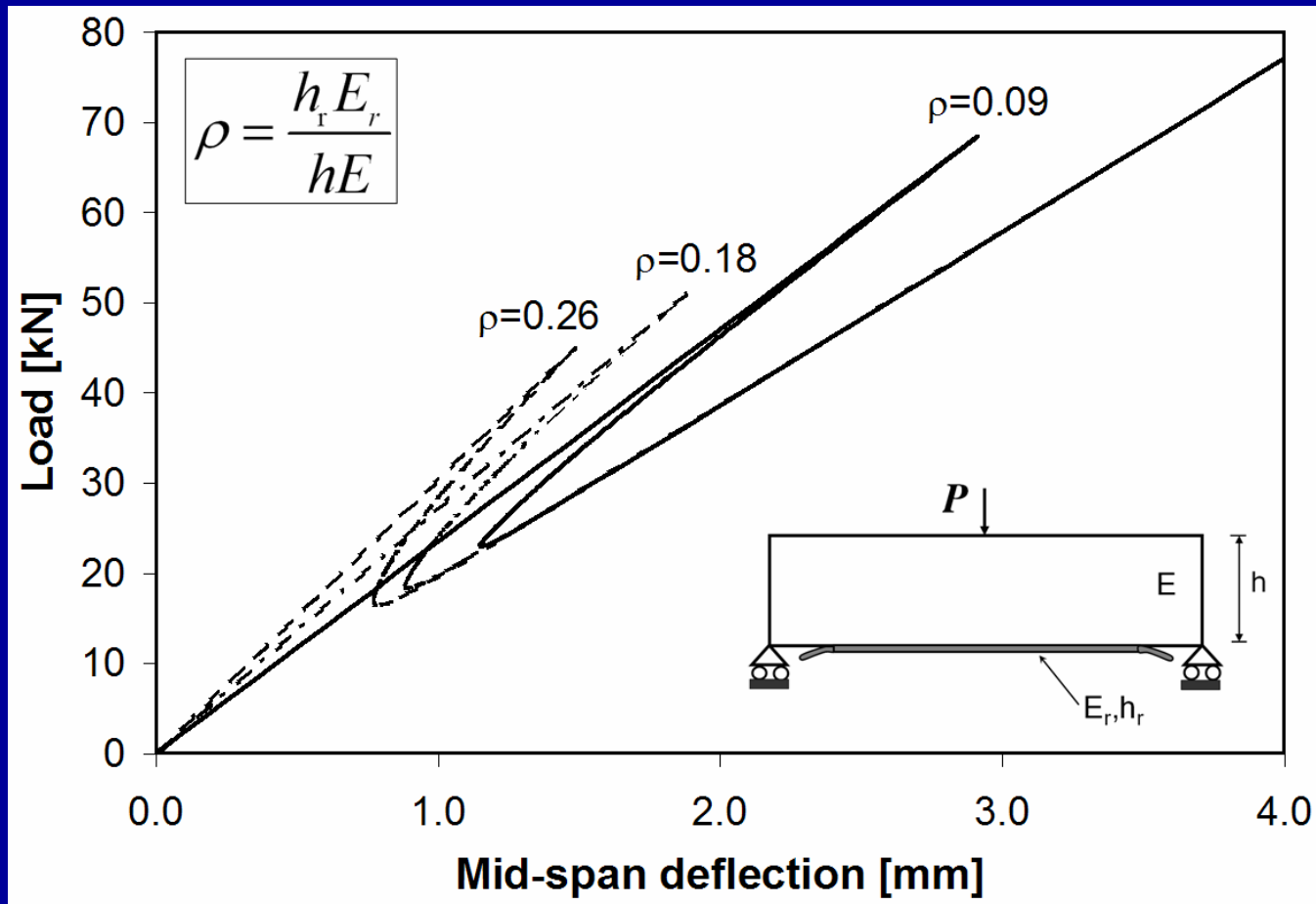
**Stress-strain curves for different values of the brittleness number:
snap-back instability occurs for inclusions with $d \gtrsim 7 \mu\text{m}$**

Snap-back instability in the delamination of retrofitted beams



Numerical vs. experimental results

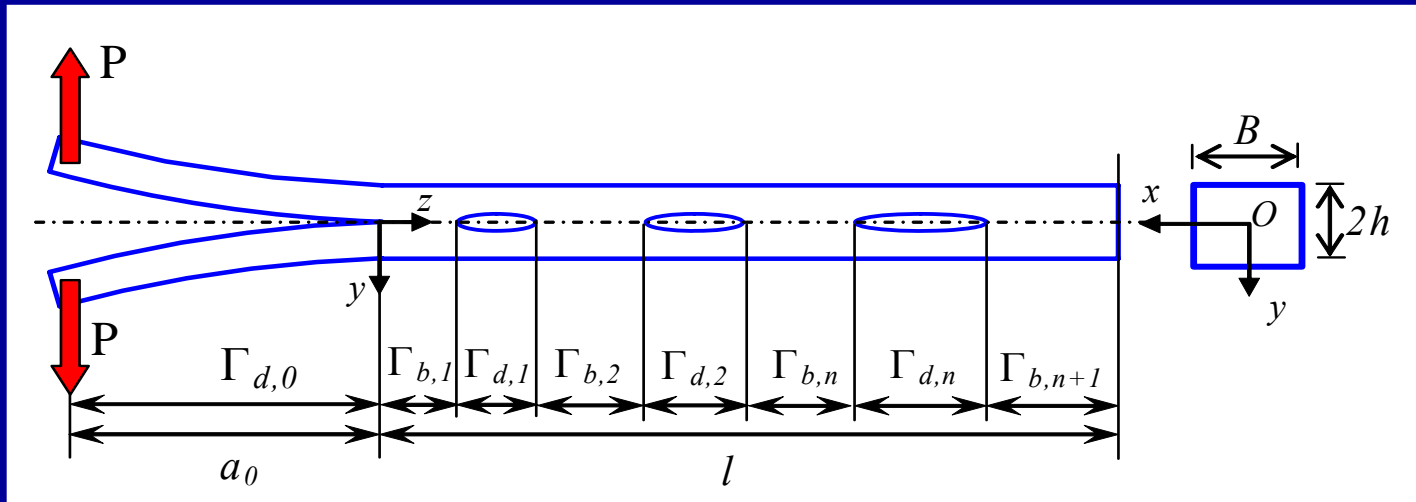
Carpinteri A., Lacidogna G., Paggi M. (2007) Acoustic emission monitoring and numerical modeling of FRP delamination in RC beams with non-rectangular cross-section, *RILEM Mat. Struct.* 40:553-566.



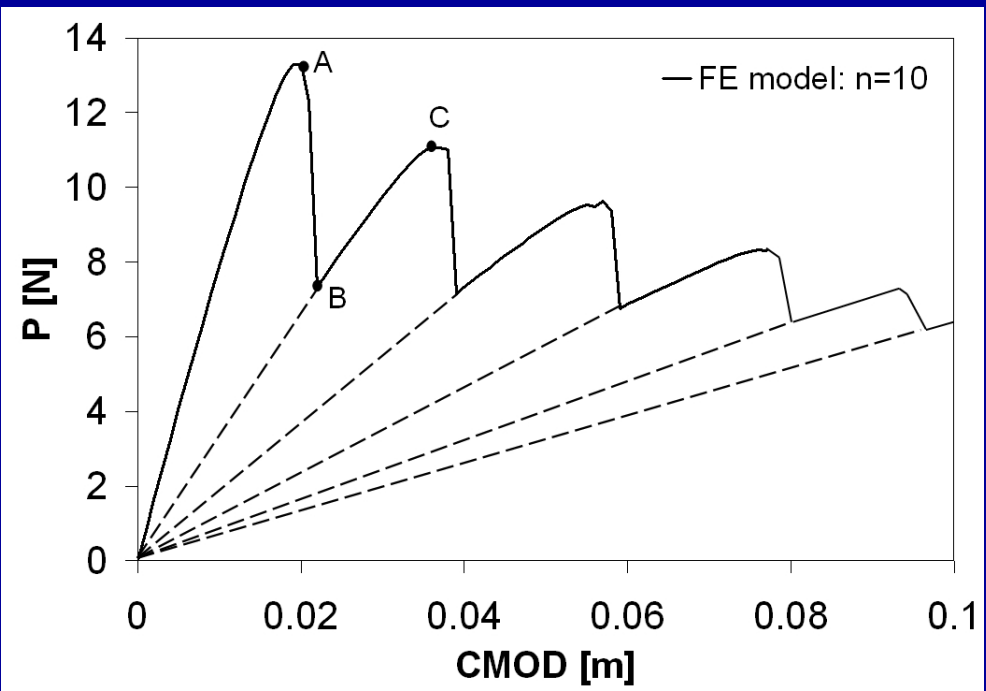
The effect of the mechanical percentage of FRP

Carpinteri A., Paggi M. Analysis of snap-back instability in the delamination of FRP-strengthened beams, *ASCE J. Engng. Mech.*, to appear.

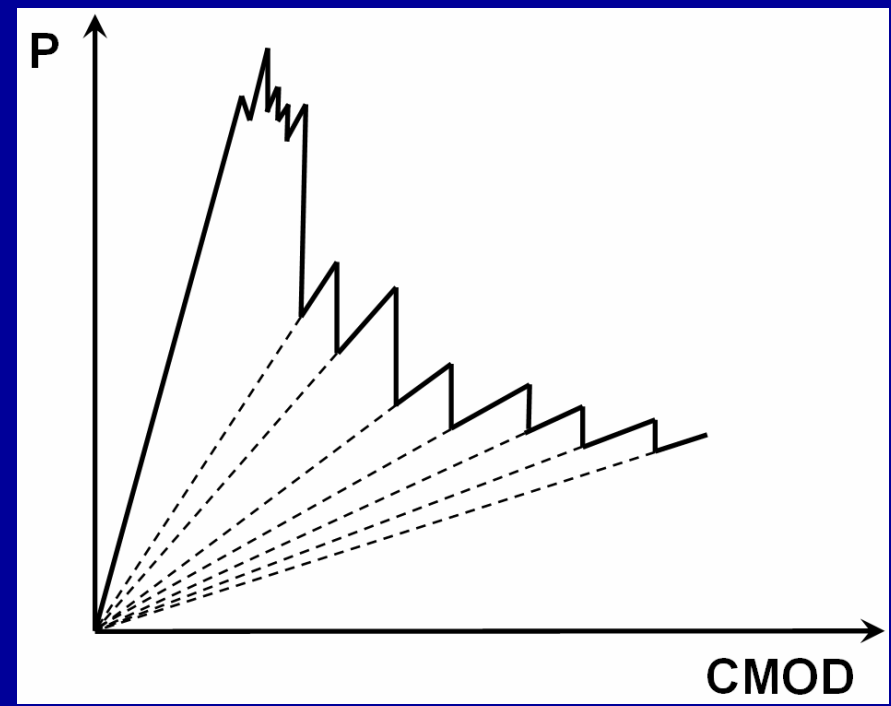
The effect of contact on the decohesion of layered beams with interfacial defects



Carpinteri A., Paggi M., Zavarise G. (2007) The effect of contact on the decohesion of laminated beams with multiple microcracks, *International Journal of Solids and Structures*, 45:129-143.



Numerical results
(10 periodically distributed defects)



Typical experimental unstable response due to nonuniform bonding